Improving Geologic and Engineering Models of Midcontinent Fracture and Karst-Modified Reservoirs Using New 3-D Seismic Attributes

Type of Report: Semiannual Scientific/Technical

Reporting Period Start Date: April 1, 2007

Reporting Period End Date: September 30, 2007

Principal Authors:

Susan E. Nissen, Consultant, McLouth, Kansas
Saibal Bhattacharya, Kansas Geological Survey, University of Kansas, Lawrence, Kansas
John Doveton, Kansas Geological Survey, University of Kansas, Lawrence, Kansas
W. Lynn Watney, Kansas Geological Survey, University of Kansas, Lawrence, Kansas

Date Report was Issued: December 2007

DOE Award Number: DE-FC26-04NT15504

Submitting Organization:

The University of Kansas Center for Research, Inc
2385 Irving Hill Road
Lawrence, Kansas 66045-7563

DISCLAIMER

This report was prepared as an account of work sponsored by an agency of the United States Government. Neither the United States Government nor any agency thereof, nor any of their employees, makes any warranty, express or implied, or assumes any legal liability or responsibility for the accuracy, completeness, or usefulness of any information, apparatus, product, or process disclosed, or represents that its use would not infringe privately owned rights. Reference herein to any specific commercial product, process, or service by trade name, trademark, manufacturer, or otherwise does not necessarily constitute or imply its endorsement, recommendation, or favoring by the United States Government or any agency thereof. The views and opinions of authors expressed herein do not necessarily state or reflect those of the United States Government or any agency thereof.

ABSTRACT

Our project goal is to develop innovative seismic-based workflows for the incremental recovery of oil from karst-modified reservoirs within the onshore continental United States. Specific project objectives are: (1) to calibrate new multi-trace seismic attributes for improved imaging of karst-modified reservoirs, (2) to develop attribute-based, cost-effective workflows to better characterize karst-modified carbonate reservoirs and fracture systems, and (3) to improve accuracy and predictiveness of resulting geomodels and reservoir simulations. In order to develop our workflows and validate our techniques, we have been conducting integrated studies, including reservoir characterization, geomodel building, and reservoir simulation, of three karst-modified reservoirs: the Permian San Andres in west Texas, the Mississippian Spergen in Colorado, and the Ordovician Arbuckle in Kansas

During this sixth reporting period, from April 1 through September 30, 2007, we have made progress toward validation of our attribute analysis techniques. We refined our reservoir characterization for the Permian San Andres study area, including mapping the configuration of the reservoir interval, summarizing porosity distribution in the reservoir, and making preliminary estimates of water saturation, directed toward building an integrated geomodel for reservoir simulation during the next reporting period. We reported our reservoir simulation results from the Mississippian Spergen study area to the field operator. Together with the operator, we decided that the simulation study will be extended to neighboring compartments in the northern portion of the Mississippian study area. The operator will conduct new well tests in the modeled compartments to confirm positions of seismically-defined flow boundaries and, if the new simulation studies successfully history match production-pressure data, the operator will drill a new infill well in the southern part of the study area based on our 3D seismic volumetric curvature analysis. For the Arbuckle study area, we determined that we have insufficient petrophysical data for generating a detailed reservoir model and insufficient production and pressure data for history matching, suggesting that reservoir simulation would produce inconclusive results. Therefore, we have determined that meaningful reservoir simulation and testing cannot be conducted for the Arbuckle study area. We identified an alternate karst-modified reservoir (to replace the Arbuckle study area) to further test our seismic volumetric curvature-based method for defining compartment boundaries. In this study area, attribute results will be validated by drilling and testing a new well in mid-2008.

Technology transfer of our project work has been accomplished through presentations at professional society meetings and postings on the project website: http://www.kgs.ku.edu/SEISKARST.

TABLE OF CONTENTS

TITLE PAGE 1

DISCLAIMER 2

ABSTRACT 3

TABLE OF CONTENTS 4

EXECUTIVE SUMMARY 5

1.0 INTRODUCTION 7

2.0 PERMIAN SAN ANDRES STUDY AREA 7

3.0 MISSISSIPPIAN SPERGEN STUDY AREA 13

4.0 ARBUCKLE STUDY AREA 14

5.0 ALTERNATE AREA FOR VALIDATING ATTRIBUTE METHODOLOGY – DICKMAN FIELD, KANSAS 15

6.0 TECHNOLOGY TRANSFER 16

7.0 CONCLUSIONS 16

LIST OF FIGURES 18

REFERENCES 20

FIGURES 21

EXECUTIVE SUMMARY

Our overall project goal is to develop seismic-based workflows for the incremental recovery of oil from karst-modified reservoirs within the onshore continental United States. In order to develop our workflows and validate our techniques, we have been conducting integrated studies of three karst-modified reservoirs: the Permian San Andres in west Texas, the Mississippian Spergen in Colorado, and the Ordovician Arbuckle in Kansas. During this sixth reporting period, from April 1 through September 30, 2007, our project was focused on the following tasks: (1) refining the reservoir characterization of the Permian San Andres study area, (2) reporting results from the Mississippian Spergen reservoir simulation to the field operator and obtaining the operator's agreement to conduct new well tests to confirm model results, (3) critically evaluating the potential for meaningful reservoir simulation in the Arbuckle study area, and (4) identifying an alternate karst-modified reservoir (to replace the Arbuckle study area) where attribute results can be validated by drilling and testing a new well.

Permian San Andres Study Area. The current focus of activity in the Permian San Andres study has been to map the configuration of the reservoir interval using seismic data and to summarize porosity distribution in the reservoir interval. The approach has included: 1) seismic mapping of the primary reservoir interval, extending from the base of the tight zone (karst) down to the "x" marker, a seismically resolvable datum at or near the base of the producing interval; 2) calculation of porosity from well logs using a mineral-porosity model, followed by calculations of porosity statistics for the reservoir interval; 3) correlation of porosity to impedance and mapping 3D seismic impedance for the reservoir interval; 4) preliminary log analysis for water saturation; and 5) comparison of results with production data to evaluate possible controls on cumulative production. Findings include: 1) several approximately north-south-trending thicks and thins in the reservoir interval are clearly visible on the seismic isochron map; 2) generally thinner karst in the structural saddle area corresponds with lower overall porosity in the underlying reservoir interval; 3) mapped porosity exhibits well developed north-south trends of high and low porosity that are essentially perpendicular to the major structure; also, a comparison of mean and center of gravity measures of porosity indicates that higher porosity is developed lower in the pay interval; 4) mean seismic impedance of the reservoir interval corresponds well with mean porosity from well logs and allows porosity approximation in areas of poor well control; 5) an initial calculation of average water saturation is consistent with the level of oil production; 6) a wide range of recoveries is noted in wells in the high volume area, but higher production generally comes from three regions: the main structural high, along the northeast flank of the main structure, and along a narrow northeast-trending area roughly corresponding to the structural saddle; and 7) a combination of factors appears to be responsible for pay distribution in the high volume area of Waddell Field. Future activities will provide more details on reservoir properties and will conclude with a reservoir simulation of a portion of the high volume area.

Mississippian Spergen Study Area. During the present reporting period, results of the characterization and simulation study of the Smoky Creek field conducted during the

previous reporting period were presented to the field operator. We decided in consultation with the operator that the simulation study will be extended to the remaining areas of the Smoky Creek field that are within the 3-D seismic survey to confirm if the compartments visible from the curvature analysis provide sufficient reserves to obtain pressure and production history matches at all the wells covered by the survey. The operator will conduct extended build-up tests on selected wells in Smoky Creek field, allowing us to estimate distance to the nearest flow boundary for comparison with the positions of seismically-defined reservoir compartment boundaries. Successful demonstration of our attribute analysis technique to delineate compartments in the Smoky Creek field will be followed by extending the analysis to the Cheyenne Wells field, located to the south. The operator will use the 3-D curvature analysis results to spot and drill an infill well in the Cheyenne Wells field some time by mid-2008, provided that the technique is able to history match production-pressure data from the Smoky Creek field. Successful production from this infill well would validate the application of our proposed attribute analysis technique to characterize compartments in this reservoir.

Arbuckle Study Area. The primary focus in the Arbuckle study during the present reporting period has been to evaluate whether seismic data correlates with reservoir porosity and to determine if there is sufficient data available for reservoir simulation. Arbuckle wells with a complete suite of well logs for generating petrophysical parameters, such as porosity and water saturation, for populating a reservoir model are sparse. In some areas, seismic impedance can be used to map lateral porosity variations. Therefore, in the Arbuckle reservoir, impedance was calculated from well logs and extracted from the seismic data and compared to porosity. Both well log impedance and seismic impedance show a poor correlation with porosity, suggesting that that the impedance may be responding to other factors in addition to porosity, such as lithological variations. The results show that seismic impedance cannot be used in the Arbuckle study area to map lateral porosity variations between well control. An added complication in this study area is that only lease production data is available, and much of the Arbuckle production is comingled with production from other reservoir intervals. This does not allow for a reliable history match for reservoir simulation. The lack of sufficient petrophysical data for generating a detailed reservoir model and the lack of production and pressure data for history matching suggest that reservoir simulation would produce inconclusive results. Therefore, we have determined that meaningful reservoir simulation and testing cannot be conducted for the Arbuckle study area.

An alternate study area (Dickman Field, Ness County, Kansas) has been identified to further test our attribute analysis technique for mapping compartment boundaries in karst-modified reservoirs. This field is expected to be a good test area because 1) a preliminary reservoir model with compartment boundaries based on seismic curvature interpretations .has already been generated, and 2) the field operator is planning to drill a new well in the field in 2008 based on curvature results, providing an opportunity for validating our model.

Technology transfer of our project work has been accomplished through presentations at professional society meetings and postings on the project website: http://www.kgs.ku.edu/SEISKARST.

1.0 INTRODUCTION

Our project goal is to develop innovative seismic-based workflows for the incremental recovery of oil from karst-modified reservoirs within the onshore continental United States. Specific project objectives are: (1) to calibrate new multi-trace seismic attributes for improved imaging of karst-modified reservoirs, (2) to develop attribute-based, cost-effective workflows to better characterize karst-modified carbonate reservoirs and fracture systems, and (3) to improve accuracy and predictiveness of resulting geomodels and reservoir simulations. In order to develop our workflows and validate our techniques, we have been conducting integrated studies of three karst-modified reservoirs: the Permian San Andres in west Texas, the Mississippian Spergen in Colorado, and the Ordovician Arbuckle in Kansas (Figure 1.1).

In the first five reporting periods, from October 1, 2004, through March 31, 2007, we (1) gathered 3-D seismic, petrophysical, and engineering data; (2) generated multi-trace seismic attribute volumes (including coherence and volumetric curvature attributes) for the 3-D seismic surveys; (3) generated a preliminary seismic attribute catalog of karst features (available online at http://www.kgs.ku.edu/SEISKARST/catalog.html); (4) conducted integrated reservoir characterization studies (seismic, geological, petrophysical, and engineering); (5) developed a workflow for geomodel building; (6) constructed a geomodel for our Mississippian Spergen study area; (7) conducted reservoir simulations for our Mississippian Spergen study area; (8) synthesized a best practices workflow for using seismic attributes (primarily geometric attributes) to characterize reservoirs modified by karst and (9) provided technology transfer through presentations at professional society meetings and associated publications, in Kansas Geological Survey Open-file reports, and via postings to our project website (http://www.kgs.ku.edu/SEISKARST).

During this sixth reporting period, from April 1 through September 30, 2007, we focused on (1) refining our reservoir characterization for the Permian San Andres study area, directed toward building an integrated geomodel for reservoir simulation during the next reporting period, (2) reporting our results from the Mississippian Spergen reservoir simulation to the field operator and obtaining the operator's agreement to conduct new well tests in the modeled compartments to confirm simulation results, (3) critically evaluating the potential for meaningful reservoir simulation in the Arbuckle study area, and (4) identifying an alternate karst-modified reservoir (to replace the Arbuckle study area) where attribute results can be validated by drilling and testing a new well. Details of the accomplishments for the April 1 through September 30, 2007 reporting period are documented below.

2.0 PERMIAN SAN ANDRES STUDY AREA

The Permian San Andres study area is approximately 5 square miles (13 square kilometers) in size and covers the "high volume area" of Waddell Field, Crane County, Texas, located on the east central flank of the Central Basin Platform of the Permian Basin. This high volume area is characterized by variable fluid production, but overall

fluid production is an order of magnitude greater than in surrounding areas of the field. A histogram of the cumulative oil and gas recovered for wells in and adjoining the high volume area in Waddell Field (Fig. 2.1) shows a wide range of recoveries between 100 M bbls and 100 MM bbls per well with nearly 50% of the wells producing 250 M BOE or less. In the high volume area, production is typically 300 M BOE and more per well (Fig. 2.2).

Reservoir heterogeneity appears to be related to stratigraphy and diagenesis, including anhydrite-cemented karst features associated with the subaerial exposure surface developed on the top of San Andres Formation. The main reservoir interval of the San Andres Formation in the high volume area has been identified as the porous zone beneath the base of the tight, anhydritic karst zone at the top of the San Andres and the "x" marker, a seismically resolvable datum that is penetrated by a majority of the wells (See June 2007 Semi-Annual Scientific/Technical Report). The map on the left of Figure 2.3 depicts the thickness of the tight interval (karst) at the top of the San Andres Formation. The karst is generally thickest on the structural highs. The map on the right of Figure 2.3 is the gross thickness of the porous interval from the base of the tight zone (base of karst) to the "x" marker. The porous interval contains both porous, grain-supported oomoldic lithofacies and non porous to low porosity mud-supported carbonate lithofacies. Thicks in the porous interval have strong northwest and northeast trends. Thicker porous intervals appear to flank the present San Andres structure. Thinner porous intervals over the structure are partly related to thicker karst, which reduced thickness of the underlying porous interval.

During the present reporting period, the focus of the Permian San Andres study has been to map the configuration of the reservoir interval using seismic data and to summarize porosity distribution in the reservoir interval. Definition of key petrophysical parameters of porosity and water saturation, as well as other parameters, within the reservoir interval will provide key inputs for reservoir simulation during the next reporting period.

2.1 Seismic mapping of the base of tight (karst) zone to "x" marker interval

Seismic horizons corresponding to the base of the tight zone and the "x" marker were interpreted across the high volume area using 3-D seismic data (See June 2007 Semi-Annual Scientific/Technical Report). A map has been generated of the isochron between these two horizons (Fig. 2.4). The isochron values are cross plotted against the isopach values generated from well tops in Figure 2.5. The correlation is generally good, suggesting that the seismic isochron can be used to approximate changes in interval thickness in locations without well control. The seismic isochron map clearly shows several approximately north-south-trending thicks and thins in the reservoir interval, which appear to swing around from a north-northeast trend in the east to a north-northwest trend in the west. The northwest trending thick suggested by the isopach map from well tops is not readily apparent in the isochron map. The isochron map also shows areas where the x marker has been truncated by the karst (white areas on the map). These areas are located on the flanks, rather than the top, of the San Andres structure (Fig. 2.4) and have a primarily north to northeast orientation. In the southern part of the map,

however, the area where the "x" marker is absent shows both a northeast trend that lines up with a saddle on the main structure and a northwest trend that parallels the main structure.

2.2 Evaluation of Porosity Distribution in the Reservoir Interval

2.2.1 Calculation of porosity from well logs

The mineral complexity of the San Andres Formation requires multiple logs in the estimation of true volumetric porosity. A mineral-porosity model was applied to the density, neutron porosity, and bulk photoelectric factor logs to solve for porosity and the results show good concordance with core-measured porosity as well as a systematic improvement on conventional cross plot porosity. Estimations of porosity from the sonic log are generally a close match with compositional porosity in zones where all the pore space is interparticle, but are underestimates in higher porosity zones where part of the pore space is vuggy or oomoldic (Fig. 2.6).

All subsequent porosity analyses make use of the compositionally corrected porosity.

2.2.2 Statistical analysis of porosity

Statistical summaries of porosity variability in the interval bounded by the base of the tight zone and the "x" marker were computed in wells logged by lithodensity-neutron measurements. In these wells, the statistics of arithmetic mean, 10th percentile (P10), and 90th percentile (P90) were generated as expressions of the average porosity and its high and low extremes. In addition, the first two moments of the porosity distribution were calculated to characterize the vertical distribution of porosity. The first moment is the center of gravity, which specifies the depth of the porosity development, while the second moment is calculated as the relative standard deviation as a measure of the depth dispersion of the porosity about the center of gravity. Details of the moment calculations are documented by Krumbein and Libby (1957).

A histogram of porosity from well #1206 (Fig. 2.7) shows a rather uniform porosity distribution with mean = 0.12, P10 phi = 0.05, P90 phi = 0.21, and standard deviation = 16.16 ft. The center of gravity for this porosity profile is at 3520 ft, the middle of the porous interval, indicating an even distribution of the porosity.

2.2.3 Lateral porosity variations

A map of mean porosity is shown on the left side of Figure 2.8. The mean porosity has clear north-south oriented highs separated by low porosity. The map of center of gravity of porosity shown on the right side of Figure 2.8 indicates both east-northeasterly and north-northwesterly patterns. The easternmost trend of high mean porosity corresponds closely to a low center of gravity suggesting a trend of better developed porosity in the lower portion of this interval. In contrast, the central low mean porosity trend corresponds to a similar trend of higher center of gravity, suggesting that the porosity has shifted to higher levels in the interval and is of lower magnitude. The westernmost north-south trend of high mean porosity corresponds closely to a low center of gravity confirming a general relationship that porosity that is developed lower in the interval is

greater in magnitude. The reason for the alternating spatial pattern of high and low porosity will be explained through further study.

The P10 and P90 porosity maps (Fig. 2.9) also depict strong north-south elongate trends, similar to the previous map of mean porosity. However, the high mean porosity trend on the west side of the mapped area closely corresponds to higher porosity on the P10 map, whereas the high mean porosity trend on the east side of the mapped area corresponds to notably high porosity values on the P90 map. The low mean porosity trend in the central mapped area is clearly lower on both the P10 and P90 maps, confirming the delineation of what appears to be distinct porosity units. Further characterization of these porosity units will be carried out in next phase of the study.

A west-east two well cross section in Figure 2.10 extends from a lower to a higher porosity area as described above. The interval from the base of the tight zone (karst) to the "x" marker thins to the east, but the amount of section with higher porosity increases. It appears that while the karst overprint has reduced porosity at the top of the San Andres Formation, intervals underlying the karst have undergone porosity enhancement. Alternatively, the lithofacies of the San Andres porous interval beneath the karst may vary from location to location (e.g., variations in grain-supported fabrics and associated mold and vug development). The parallel nature of the Top of San Andres and the "x" marker are indicative of their depositional origin, while the angular nature of the base of the tight zone relative to these two datums is reflective of its diagenetic origin.

The index map in Figure 2.10 shows the line of section on a structure map on top of the San Andres Formation overlain with black contours of the P90 porosity. Note that the low porosity contours are subparallel to the north-northeast-trending saddle in the structure. The saddle area also has a thinner karst interval, thus the upper section of San Andres Formation is differentially preserved, and as the maps have indicated, the area has lower values of porosity.

2.2.4 Correlation of porosity to impedance

Areas of higher porosity and more favorable reservoir quality are likely detectable on seismic as areas of low impedance. Impedance was calculated for well #1261 using bulk density x sonic velocity derived from logs and was compared to core porosity (Fig. 2.11). At this scale of measurement the empirical correlation between impedance and porosity is high, $r^2 = 0.79$, and suggests a high potential in using seismic impedance to examine porosity distribution, in spite of complex lithologies and pore types.

Impedance was then computed for all wells containing sonic and density logs, and mean impedance was calculated for the base tight to "x" marker interval. This mean log impedance has been compared to the mean porosity for the same interval. Figure 2.12 shows that the mean log impedance and mean porosity are well correlated.

Mean impedance was also generated from the seismic data for the interval between the base tight horizon and the "x" marker horizon (Fig. 2.13). This mean seismic impedance is also cross plotted against mean porosity in Figure 2.12. Although there is more scatter

than for the log data, the seismic data show the same trend of decreasing porosity with increasing impedance. This correlation between impedance and porosity allows us to use the seismic impedance map in Figure 2.13 to approximate the distribution of mean porosity in areas with poor well control.

2.3 Preliminary Log Analysis for Water Saturation

During the next reporting period, we will conduct a detailed reservoir characterization of a selected area to derive parameters needed for reservoir simulation. As a preliminary step, water saturation calculations were performed on well #1206 in the northeastern map quadrant. PfEFFER software was used with the Archie equation to calculate a water saturation profile for the porous San Andres Formation extending from the base of the tight zone (karst) down to the "x" marker. The compositionally corrected porosity was used in the calculation. A formation water resistivity, R_w, of 0.065 was provided by the operator. Due to the variable nature of the pore type including a dominance of moldic and vuggy pores, a variable cementation exponent, m, was empirically calculated using the Nugent Equation (Nugent, 1984), m = 2 x log (sonic ϕ)/log (total ϕ). The average m determined using this method is 2.35.

While preliminary, the depth profiles of the reservoir interval in well #1206 show relatively low log calculated water saturation (average 0.46), which would be expected with the large amount of oil and gas that has been recovered from this perforated interval (over 300 M BOE) (Figure 2.14). The porosity profile in well #1206 shows an overall upward increase in porosity from the base of the interval to mid way in the profile. This is then overlain by a decreasing trend, possibly indicating a pattern of deposition. The profile of the cementation exponent of the Archie equation, m, calculated using the Nugent Equation is lower, around 2, near the base of the porous interval, but increases upward to the mid section where porosity is highest. The cementation exponent then decreases slightly below the base of the tight, karsted interval that immediately overlies the reservoir. The higher m value, averaging 2.35, is likely an indication of increased moldic and vuggy porosity. An analysis of the porosity log suites in this well confirms that estimated vug porosity increases with higher values of total porosity (Figure 2.14), a relationship that we have observed in other reservoirs dominated by moldic porosity (Byrnes, et al., 2003, http://www.kgs.ku.edu/PRS/publication/2003/ofr2003-32/index.html).

2.4 Possible Controls on Cumulative Production

The high-volume area of Waddell Field is denoted by high cumulative oil and gas production, expressed by a map of barrels of oil equivalent (BOE) (Fig. 2.15). A conversion factor of 5.7 MCF gas to one equivalent bbl of oil is used in the conversion to BOE. The bright green to red areas in Figure 2.15 identify elevated cumulative production (in excess of 300,000 BOE). In addition to high production (in excess of 600,000 BOE) associated with the structural high in the northwestern quadrant of the map, there is a narrow, northeast-trending area of elevated cumulative production near the center of the map that appears to correspond roughly to the location of the saddle on

the structural high. Cumulative gas production and total fluid (oil+gas+water) produced are also shown in Figure 2.15. These maps show the same general high volume area of Waddell Field, but details within the high volume area are different from the cumulative oil and gas production map. Both the cumulative gas production and total fluid production maps reveal similar northwest and northeast trending, high-volume production anomalies. These anomalies are in roughly similar locations on the two maps. The northeast-trending area of high production on these maps coincides with the saddle on the San Andres structural high. The northwest-trending high production area is located along the northeastern flank of the main structural high. The cause of this empirical relationship between structure and production is yet to be determined.

Figure 2.16 shows the production as compared to the isochron of the base tight to "x" marker reservoir interval. The most significant relationship seen on these maps is that areas of high cumulative gas production coincide with areas where the base tight to "x" marker isochron is thin, particularly along the saddle in the San Andres structure map.

Contours of the mean porosity of the interval below the tight zone and above the "x" marker are superimposed on the production maps in Figure 2.17 and show that there is not a clear relationship between porosity and production. Obviously other factors are involved. For one, the simple statistics that summarize the porosity do not reflect actual net effective porosity, permeability, and water saturation. Also, potential reservoir compartmentalization, as suggested by the network of black lineaments on the most negative curvature map extracted along the "x" marker (Fig. 2.18), that may represent fractures, can impact production. Finally, it should be noted that the cumulative production for this field may be somewhat misleading with regard to reservoir properties, as some of the wells were temporarily converted to injection wells, then put back on line as producers later.

2.5 Discussion

A common conclusion reached by studies characterizing reservoirs in the San Andres Formation is that substantial heterogeneities have limited oil production from primary and secondary recovery methods to roughly 30% OOIP (Ruppel and Cander, 1988). Lithofacies, namely successions of discontinuous carbonate grainstone deposits comprise depositional cycles and cycle sets. Porosity in these deposits is greatly affected by differential dissolution and cementation leading to notable vertical and horizontal compartmentalization. Of late, the role of structural deformation has been increasingly recognized as significant in fields that produce from the San Andres Formation. Specifically, partial sealing faults and fractures, both artificial and natural have compartmentalized the reservoir and strongly influenced production at Vacuum and Olson Fields in West Texas (Pranter et al., 2004; Hurley and Ustabas, 2004). Three dimensional seismic and horizontal wells have been used to target and drain resulting reservoir compartments.

Faults studied in Vacuum Field are partial sealing and low displacement (<25 ft). They offset and isolate the thin depositional cycles that range from several feet to over 10 ft in

thickness. Seismic coherence was used to map the faults in Vacuum Field to help design trajectories of horizontal wells, resulting in orders of magnitude increases in production (Hurley and Ustabas, 2004). It should be noted that the volumetric curvature attributes that we are using in our study have been shown to image small offset faults and fractures much better than coherence (e.g., Al-Dossary and Marfurt, 2006). A horizontal well was also successfully drilled in the Olson Field, a depleting field where pressure and waterflood response showed poor communication between offset wells. In Olson Field, a horizontal well intersected an old hydrofrac, resulting in a ~10-fold increase in oil production in the offset vertical well from which the hydrofrac originated. The horizontal well apparently contacted previously untapped porous stratal units, which then were drained by via the hydrofrac by the vertical well. Nearby pressure interference testing confirms a narrow west-northwest trend of high-permeability and an inferred natural fracture (1 mi long). The trends of both the natural and induced fractures are roughly parallel to the regional stress field (west-east) (Pranter et al., 2004). Other studies of San Andres reservoir, such as in Keystone Field, have identified fracture sets as important to reservoir performance (Major and Holtz, 1997).

Similarly, in our current investigation, the influence of structural deformation, including probable fracture sets and local folding, is being made apparent through analysis of seismic attributes, subsurface mapping, and well tests. Analysis of well log data further suggests that the karst overprinting and porosity distribution are also closely related to larger scale structural deformation. While much of the porosity is secondary, the porous intervals are usually grain-supported fabrics, where grains (ooids) were preferentially dissolved. Intermediate results reported here indicate that the distribution of the grainstone shoals themselves may be closely associated with topography, at least partially caused by contemporaneous structural deformation. Thus, a combination of factors appear be responsible for pay distribution in the high volume area of Waddell Field.

3.0 MISSISSIPPIAN SPERGEN STUDY AREA

The Mississippian study area is located in Cheyenne Wells and Smoky Creek fields (Fig. 3.1) in Cheyenne County, Colorado, where oil is produced from the Mississippian Spergen reservoir. Based on standard well-level log analysis and 40-acre drainage, many wells showed high (> 45%) to greater than 100% recovery, thus leading to the question – are the wells draining uneven compartments? 3-D seismic volumetric curvature analysis carried out earlier in this project revealed the possible presence of reservoir compartments. To validate if lineaments interpreted from the curvature attributes were attributable to compartment boundaries, reservoir simulation of one of the larger compartments in Smoky Creek field, with two productive wells, was carried out. As reported in the June 2007 Semi-Annual Scientific/Technical Report, these simulation studies resulted in reasonable matches with production and pressure histories for the two wells, assuming that the boundaries visible on the 3-D attribute map were no-flow boundaries.

During the present reporting period, results of the characterization and simulation study of the Smoky Creek field were presented to the field operator, Mull Drilling Co. (MDC)

– one of the industry partners in this project. We decided in consultation with MDC that the current simulation study would be extended over the remaining areas of the Smoky Creek field that were within the 3-D seismic survey to confirm if the compartments visible from the curvature analysis provided sufficient reserves to obtain pressure and production history matches at all the wells covered by the survey (Fig. 3.2). MDC has agreed to conduct extended build-up tests in selected wells, which will allow us to estimate distance to the nearest flow boundary for comparison with the positions of seismically-defined reservoir compartment boundaries.

Successful demonstration of our attribute analysis technique to delineate compartments in the Smoky Creek field would be followed by extending the analysis to the Cheyenne Wells field, located to the south. MDC plans to use the 3-D attribute analysis to spot and drill an infill well in the Cheyenne Wells field some time by mid-2008, provided that the technique is able to history match production-pressure data from the Smoky Creek field. Successful production from this infill well would validate the application of our proposed attribute analysis technique to characterize compartments in fracture and karst-modified reservoirs.

4.0 ARBUCKLE STUDY AREA

The Arbuckle study area, in Russell County, Kansas, is a 9 mi^2 (23 km^2) area covered by a 3-D seismic survey (Fig. 4.1). In this study area, the Arbuckle reservoir sits at or near a pre-Pennsylvanian unconformity and karst surface, and Arbuckle production is located on local remnant highs. As noted in previous reports, shallow penetration of the Arbuckle (<12 ft (4 m) in a significant number of wells) and limited well log data make it difficult to characterize the Arbuckle reservoir from well data alone.

During the present reporting period, we attempted to tie reservoir properties in the Arbuckle study area to our available seismic data. We begin by testing the relationship between seismic impedance and porosity in the Arbuckle reservoir using well log data. One well in the study area with a sonic log also contains neutron and density logs. This well (well #1) only penetrates 10 ft below the top of the Arbuckle, so there are a limited number of data points for our analysis. Impedance at each log sample is calculated using the sonic and density logs and is cross plotted against the average of neutron and density porosity in Figure 4.1. There is a general trend of decreasing porosity with increasing impedance, but the correlation is low ($r^2 = 0.295$), suggesting that the impedance within the Arbuckle reservoir may be responding to other factors in addition to porosity, such as lithological variations.

In order to test whether there might be a better correlation using mean porosity over a thicker interval and impedance extracted from the seismic data, mean seismic impedance within the interval from 0-4 ms below the top of the Arbuckle (corresponding roughly to an interval approximately 30 ft (9 m) thick) was generated. A map of the mean seismic impedance is shown in Figure 4.2. Mean porosity was calculated for this same interval for the 8 wells in the study area with neutron-density porosity. Mean porosity is cross plotted against seismic impedance in Figure 4.3. This plot shows no apparent empirical

relationship between the seismic impedance and porosity, confirming that seismic impedance cannot be used in the Arbuckle study area to map lateral porosity variations between well control.

The sparse distribution of reliable porosity (and other key petrophysical parameters) from well logs and the inability to use seismic data to define lateral porosity variations makes it impossible to build a reliable detailed reservoir model for the Arbuckle study area.

As stated in the June 2007 Scientific/Technical Report, an added complication in this study area is that only lease production is available, and much of the production is comingled. This does not allow for a reliable history match for the reservoir simulation.

Because of the lack of sufficient petrophysical data for generating a detailed reservoir model and the lack of production and pressure data for history matching, any simulation of the reservoir compartmentalization indicated by seismic curvature analysis would produce inconclusive results. Therefore, we have determined that meaningful reservoir simulation and testing cannot be conducted for the Arbuckle study area.

5.0 ALTERNATE AREA FOR VALIDATING ATTRIBUTE METHODOLOGY – DICKMAN FIELD, KANSAS

Dickman field, a karst-modified Mississippian field in Ness County, Kansas, has been previously studied and characterized by the Kansas Geological Survey (KGS). A preliminary reservoir model was developed for this field using 3-D seismic volumetric curvature attributes. This reservoir model suggests that fracture and karst processes produced reservoir compartments bounded by non-flow boundaries oriented in one geographic direction and permeable boundaries oriented along the orthogonal direction (Fig. 5.1). Wells located near the permeable boundaries were characterized by high water production while wells located away from the non-flow boundaries were characterized by relatively higher oil production (Fig. 5.2) (Nissen et al., 2004).

Study results of the Dickman field were presented to Grand Mesa Operating Co. (GMOC) - the field operator, and GMOC plans to spot its next infill well in the Dickman field based on the 3-D curvature map. Currently, it is carrying out negotiations with its lease partners to complete the necessary legal formalities. GMOC expects to commence its drilling operations by mid-2008.

As a part of this project, the infill well will be cored, drill stem tested, and produced. KGS will carry out a 1-well simulation study of the infill well to history match its performance given the compartment boundaries around the well as defined from the 3-D attribute analysis. A match between simulated and observed production/pressure performance will validate the effectiveness of our proposed attribute analysis technique for mapping compartment boundaries in karsted reservoirs.

6.0 TECHNOLOGY TRANSFER

The following papers were presented at the 2007 AAPG Mid-Continent Meeting, September 9-11, Wichita, KS:

Carr, T. R., and S. E. Nissen, Application of curvature attributes to Kansas subsurface data.

Nissen, S. E., E. C. Sullivan, K. J. Marfurt, and T. R. Carr, Improving reservoir characterization of karst-modified reservoirs with 3-D geometric seismic attributes.

The following abstract has been accepted for presentation at the 2008 AAPG Annual Meeting, April 20-23, San Antonio, TX:

Nissen, S. E., J. H. Doveton, and W. L. Watney, Petrophysical and Geophysical Characterization of Karst in a Permian San Andres Reservoir, Waddell Field, West Texas

In addition, information related to the project (including project background, personnel, a catalog of seismic karst features, publications, and semi-annual scientific/technical reports) is posted to our project website: http://www.kgs.ku.edu/SEISKARST.

7.0 CONCLUSIONS

San Andres study area

Findings in the current phase of the project include the following:

- Seismic isochron mapping closely correlates with thickness data derived from logs.
- There are several approximately north-south-trending thicks and thins in the reservoir interval.
- Generally thinner karst in the structural saddle area corresponds with lower overall porosity in the underlying reservoir interval.
- Porosity maps exhibit well developed north-south trends of high and low porosity that are essentially perpendicular to the major structure; also, a comparison of mean and center of gravity measures of porosity indicates that higher porosity is developed lower in the pay interval.
- The mean seismic impedance of the reservoir interval corresponds well with mean porosity from well logs and allows porosity approximation in areas of poor well control.
- An initial calculation of average water saturation is consistent with the level of oil production. A variable cementation exponent, m, was used, derived from the Nugent Equation. The average m of 2.35 is consistent with moldic porosity that dominates this reservoir.
- A wide range of recoveries is noted in wells in the high volume area. Higher production generally comes from 1) the main structural high, 2) along the

northeast flank of the main structure, and 3) along a narrow northeast-trending area roughly corresponding to the structural saddle.

- A combination of factors appears to be responsible for pay distribution in the high volume area of Waddell Field.

Future activities will provide more details on reservoir properties and will conclude with a reservoir simulation of a portion of the high volume area.

Mississippian study area

During the present reporting period, results of the characterization and simulation study of the Smoky Creek field were presented to the field operator, resulting in the following action items:

- The current simulation study will be extended over the remaining areas of the Smoky Creek field that are within the 3-D seismic survey to confirm if the compartments visible from the curvature analysis provide sufficient reserves to obtain pressure and production history matches at all the wells covered by the survey.
- The field operator will conduct extended build-up tests in selected wells, allowing us to estimate distance to the nearest flow boundary for comparison with the positions of seismically-defined reservoir compartment boundaries.
- The field operator will use the 3-D curvature analysis results to spot and drill an infill well in the Cheyenne Wells field some time by mid-2008, provided that the technique is able to history match production-pressure data from the Smoky Creek field.

Arbuckle study area

- No correlation can be identified between impedance extracted from the seismic data volume and porosity for the Arbuckle reservoir.
- There is insufficient petrophysical data for generating a detailed reservoir model and insufficient production and pressure data for history matching in the Arbuckle study area. Therefore, any reservoir simulation incorporating the compartmentalization indicated by seismic curvature analysis would produce inconclusive results.

An alternate study area (Dickman Field, Ness County, Kansas) has been identified to further test our attribute analysis technique for mapping compartment boundaries in karst-modified reservoirs. This field is expected to be a good test area because:

- A preliminary reservoir model with compartment boundaries based on seismic curvature interpretations .has already been generated.
- The field operator is planning to drill a new well in the field in 2008 based on curvature results, providing an opportunity for validating our model.

LIST OF FIGURES

Figure 1.1 Index map showing locations of study areas 21

Figure 2.1 Histogram of cumulative oil and gas production in and adjoining the high volume area of Waddell Field.....21

Figure 2.2 Subsea depth map of the top of the San Andres Formation in the high volume area of Waddell Field.....22

Figure 2.3 Left: Isopach map of upper tight zone of San Andres Formation interpreted as karst, with top of San Andres Formation subsea depth contours superimposed. Right: Isopach map of the interval from the base of the tight zone to the "x" marker. 23

Figure 2.4 Seismic isochron map (in two-way travel time) of the interval from the base of the tight zone to the "x" marker. Isopach contours of the same interval from well tops are superimposed on the left and top of San Andres subsea depth contours are superimposed on the right. 23

Figure 2.5 Cross plot of isopach vs. seismic isochron for the base tight to x marker interval. 24

Figure 2.6 Cross plot of core porosity versus multimineral porosity and sonic porosity in well #1261. 24

Figure 2.7 Histogram of corrected porosity for the porous interval from base of tight zone to "x" marker in well #1206.....25

Figure 2.8 Mean porosity (left) and center of gravity of porosity (right). 25

Figure 2.9 10th percentile (P10) porosity map (left) and 90th percentile (P90) porosity map (right). 26

Figure 2.10 Structural wireline log cross section including wells #1220 and #1206. Index map shows top of San Andres structure overlain with P90 porosity contours.....26

Figure 2.11 Cross plot of core porosity and well log impedance for well #1261. ..27

Figure 2.12 Cross plot of mean porosity versus mean impedance from well logs (red) and from seismic data (blue) for the interval between the base of the tight (karst) zone and the "x" marker.....27

Figure 2.13 Map of mean seismic impedance for the interval from the base of the tight zone to the "x" marker. Mean porosity contours from well logs are superimposed. 28

Figure 2.14 Petrophysical profile for well #1206 and cross plot of vug porosity vs. total porosity. 29

Figure 2.15 A) Cumulative oil and gas map in BOE. B) Cumulative total fluid (oil+gas+water) map in BOE. C) Cumulative gas map in BOE. All maps are superimposed with contours of the top of San Andres subsea depth structure.....30

Figure 2.16 Isochron of the reservoir interval from the base of the tight karst zone to the "x" marker overlain by bubbles of A) cumulative oil and gas in BOE; B) cumulative total fluid (oil+gas+water) in BOE; and C) cumulative gas in BOE. 31

Figure 2.17 A) Cumulative oil and gas map in BOE. B) Cumulative total fluid (oil+gas+water) map in BOE. C) Cumulative gas map in BOE. All maps are superimposed with contours of mean porosity for the base tight to "x" marker interval. 32

Figure 2.18 Most negative volumetric curvature extracted along the "x" marker horizon. 33

Figure 3.1 Structure map of the top of Spergen in the Mississippian study area, enhanced by seismic control within the 3D seismic outline... 34

Figure 3.2 Most positive curvature map extracted along the approximate level of the top of Spergen for southern Smoky Creek field. Potential reservoir compartments are outlined. 35

Figure 4.1 Cross plot of neutron-density porosity versus well log impedance in well #1.....36

Figure 4.2 Map of mean seismic impedance for the interval from 0 to 4 ms below the top of Arbuckle horizon. 37

Figure 4.3 Cross plot of mean neutron-density porosity for the interval from 0 to 30 ft (9 m) below the top of the Arbuckle versus mean seismic impedance for the interval from 0 to 4 ms below the interpreted Arbuckle horizon. 38

Figure 5.1 Most negative curvature map for the Mississippian in Dickman Field. 39

Figure 5.2 Cross plots of 5-year oil and water production versus distance to northeast-trending and northwest-trending curvature lineaments.....40

REFERENCES

Al-Dossary, S., and Marfurt, K. J., 2006, 3-D volumetric multispectral estimates of reflector curvature and rotation: Geophysics, v, 71, p. P41-P51.

Hurley, N.F., and Ustabas, S., 2004, Incremental oil recovery using a horizontal drainhole in the San Andres Formation, Olson field, West Texas: AAPG Bulletin, v., 88, p. 133-151.

Krumbein, W.C., and Libby, W. G., 1957, Application of moments to vertical variability maps of stratigraphic units: AAPG Bull., v. 41, no. 2, p.197-211.

Major, R.P., and Holtz, M.H., 1997, Identifying fracture orientation in a mature carbonate platform reservoir: AAPG Bulletin, v. 81, p. 1063-1069.

Nissen, S. E., Marfurt, K. J., and Carr, T. R., 2004, Identifying subtle fracture trends in the Mississippian saline aquifer unit using new 3-D seismic attributes: Kansas Geological Survey Open-File Report 2004-56, http://www.kgs.ku.edu/PRS/publication/2004/2004-56/.

Nugent, W.H., 1984, Letters to the Editor: The Log Analyst, v. 25, no. 2, p. 2-3.

Pranter, M. J., N. F. Hurley, T. L. Davis, M. A. Raines, and S. C. Wehner, 2004, Dual-lateral horizontal wells successfully target bypassed pay in the San Andres Formation, Vacuum Field, New Mexico: AAPG Bulletin, vol. 88, p. 99-113.

Ruppel, S.C., and Cander, H.S., 1988, Effects of facies and diagenesis on reservoir heterogeneity: Emma San Andres Field, West Texas: Bureau of Economic Geology: Report of Investigations, No. 178, 67 p.

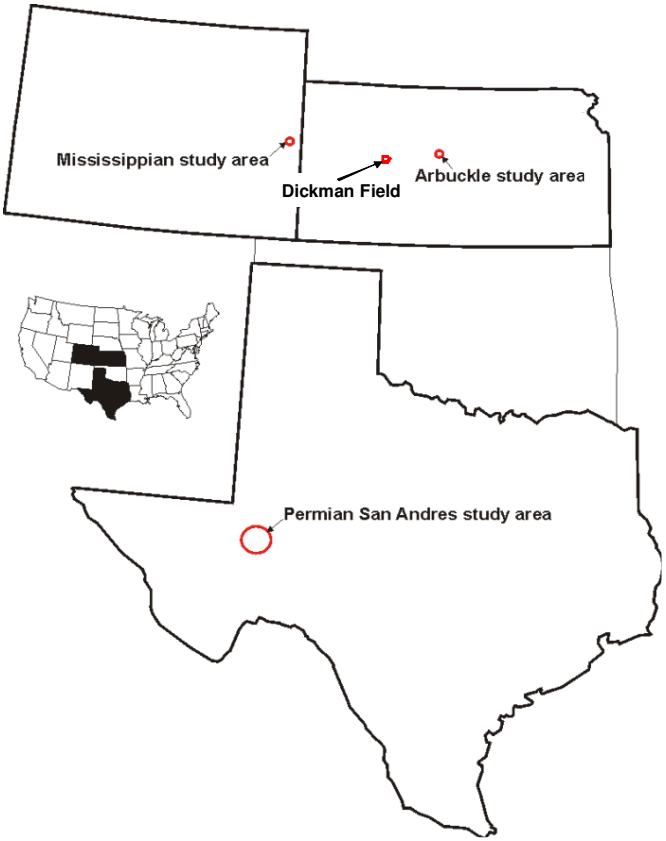

Figure 1.1. Index map showing locations of study areas. Dickman field, an alternate study area discussed later in the text, is also shown.

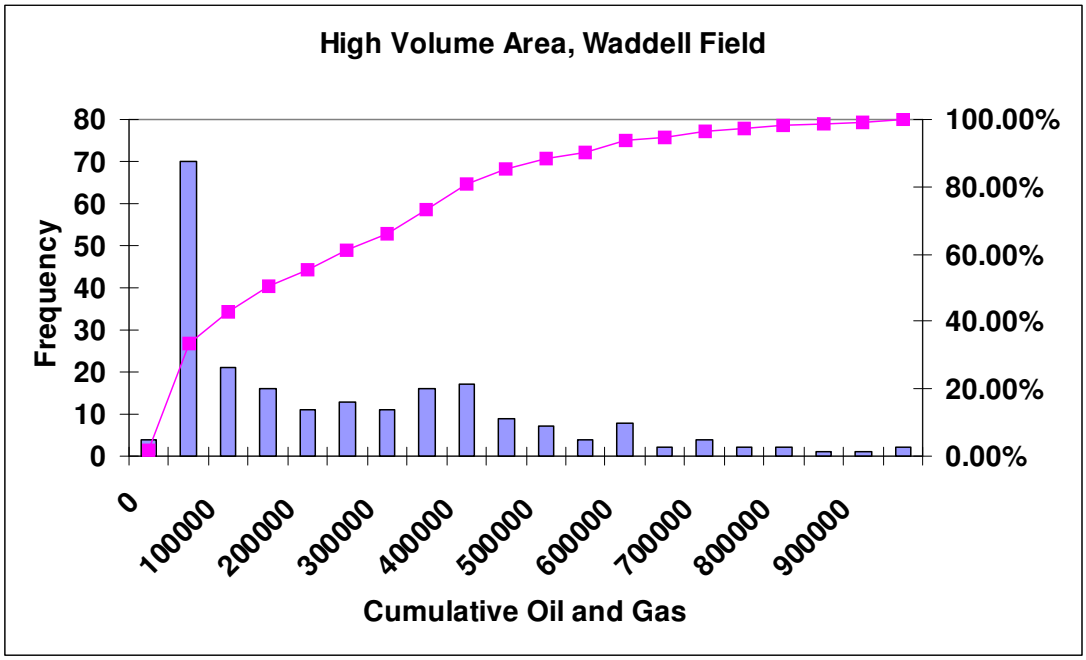

Figure 2.1. Histogram of cumulative oil and gas production in and adjoining the high volume area of Waddell Field.

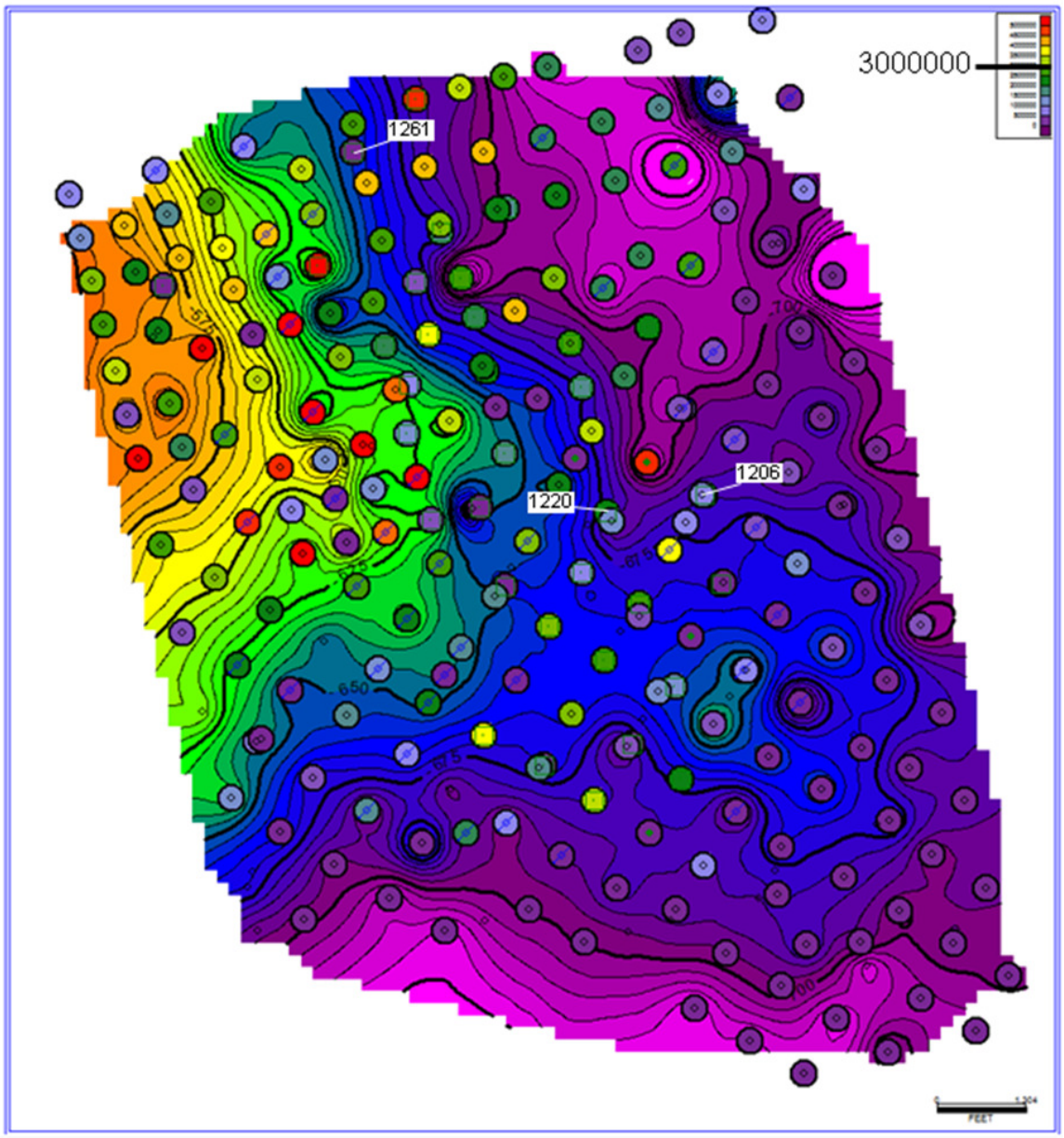

Figure 2.2. Subsea depth map of the top of the San Andres Formation in the high volume area of Waddell Field. Bubbles show cumulative oil and gas production in BOE. Wells discussed in the text are labeled.

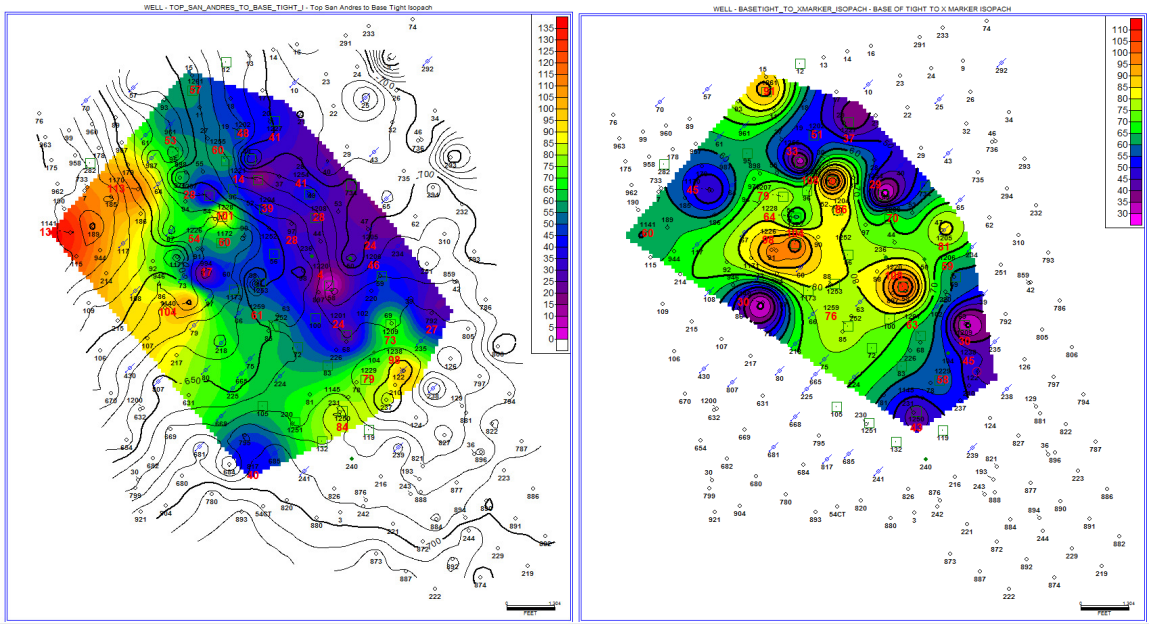

Figure 2.3. Left: Isopach map of upper tight zone of San Andres Formation interpreted as karst, with top of San Andres Formation subsea depth contours superimposed. Right: Isopach map of the interval from the base of the tight zone to the "x" marker.

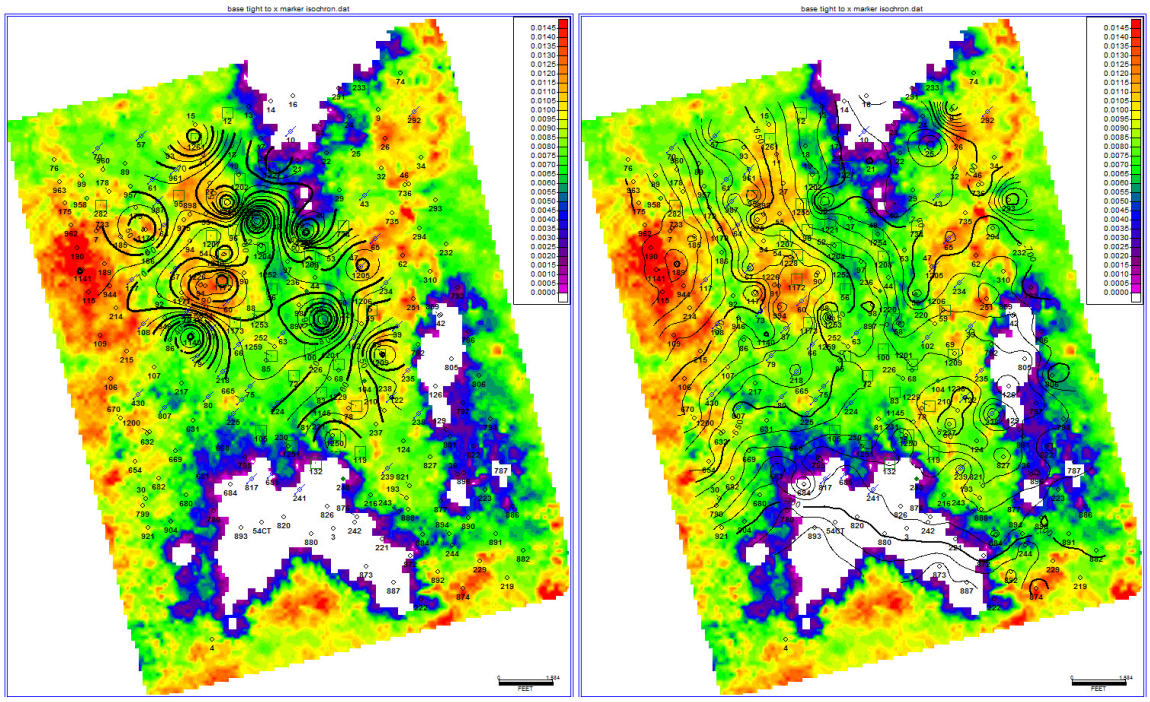

Figure 2.4. Seismic isochron map (in two-way travel time) of the interval from the base of the tight zone to the "x" marker. Isopach contours of the same interval from well tops are superimposed on the left and top of San Andres subsea depth contours are superimposed on the right.

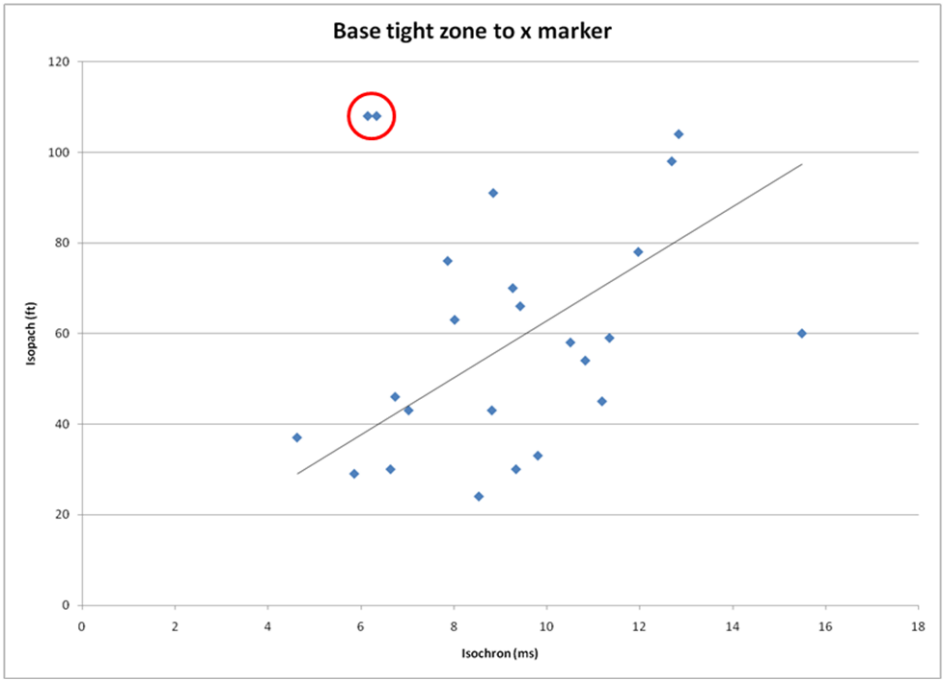

Figure 2.5. Cross plot of isopach vs. seismic isochron for the base tight to x marker interval. The correlation is generally good. The two outliers circled in red at the top of the plot are locations where the "x" marker picks in the wells are questionable and may need to be adjusted.

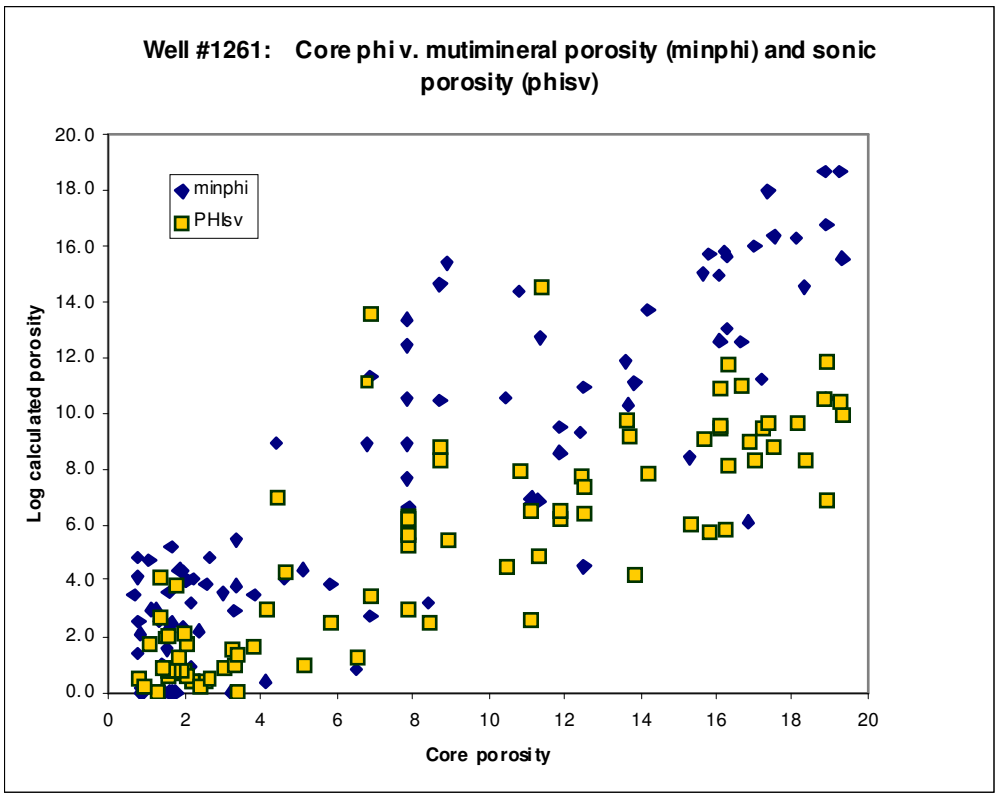

Figure 2.6. Cross plot of core porosity versus multimineral porosity and sonic porosity in well #1261. The porosity estimations from the sonic log are generally a close match with compositional porosity in zones where all the pore space is interparticle, but sonic porosities are underestimates in higher porosity zones where part of the pore space is vuggy or oomoldic.

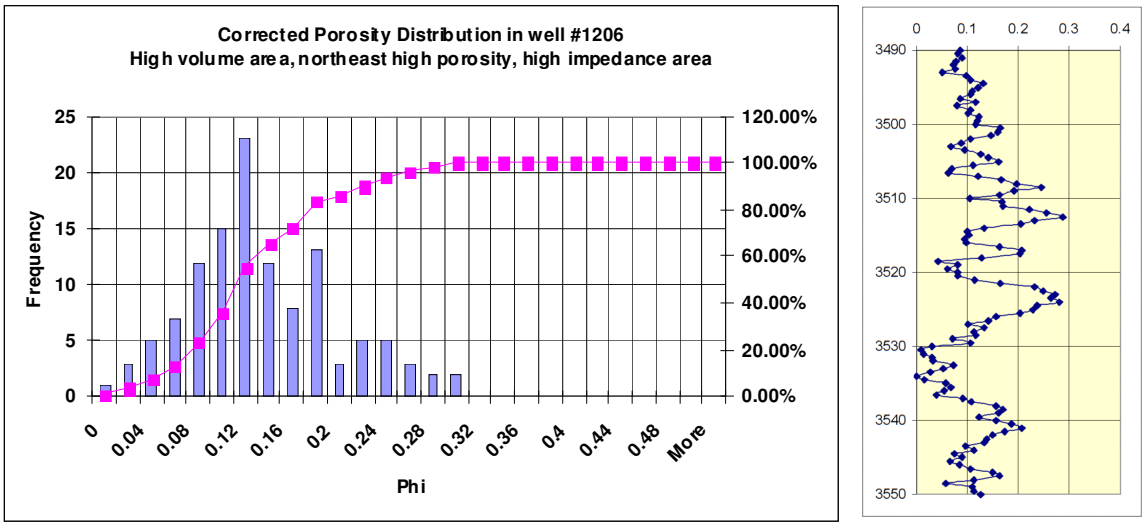

Mean = 0.12, 10th percentile phi = 0.05,
90th percentile phi = 0.21
Standard deviation = 16.16

Figure 2.7. Histogram of corrected porosity for the porous interval from base of tight zone to "x" marker in well #1206.

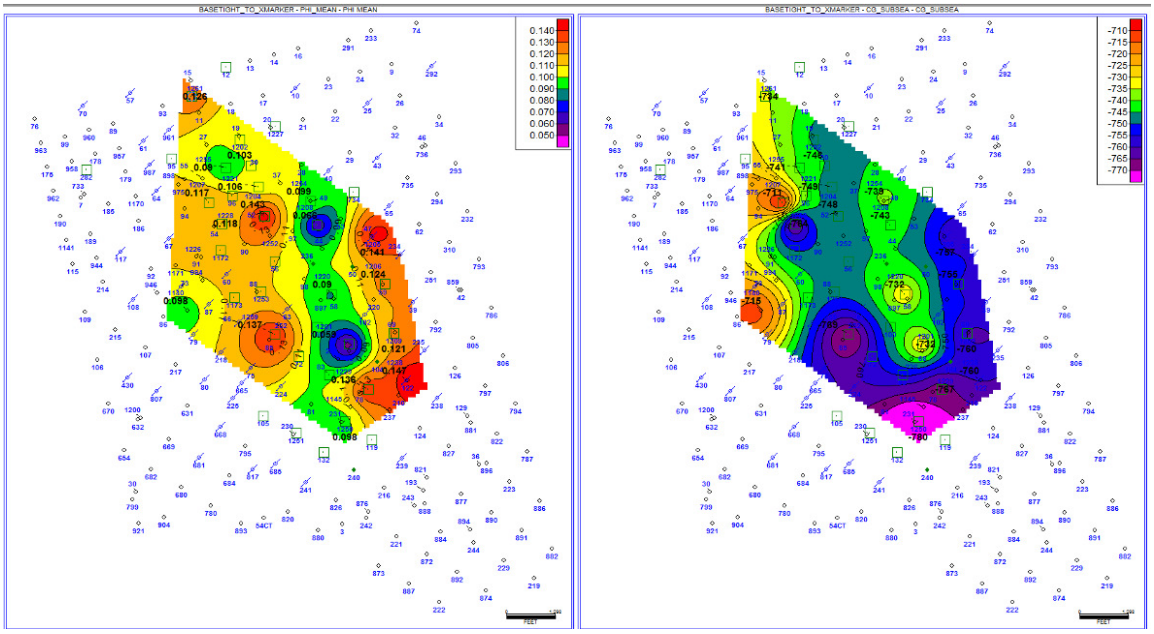

Figure 2.8. Mean porosity (left) and center of gravity of porosity measured in feet subsea (right). Mean porosity has clear N-S oriented highs (orange to red) separated by low porosity (green to blue). Lower center of gravity (blue) corresponds to higher mean porosity.

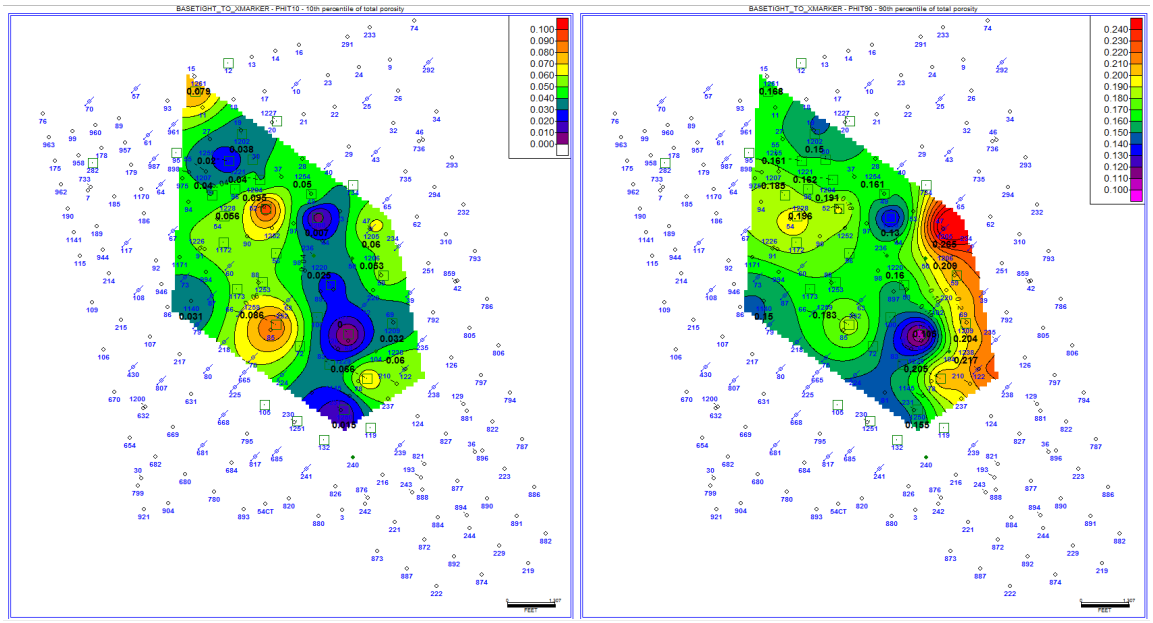

Figure 2.9. 10th percentile (P10) porosity map (left) and 90th percentile (P90) porosity map (right). P10 porosity is generally higher where P90 porosity is higher; however P10 porosity is highest along a N-S trend on the west side of the mapped area while P90 porosity is highest along a N-S trend on the east side of the mapped area.

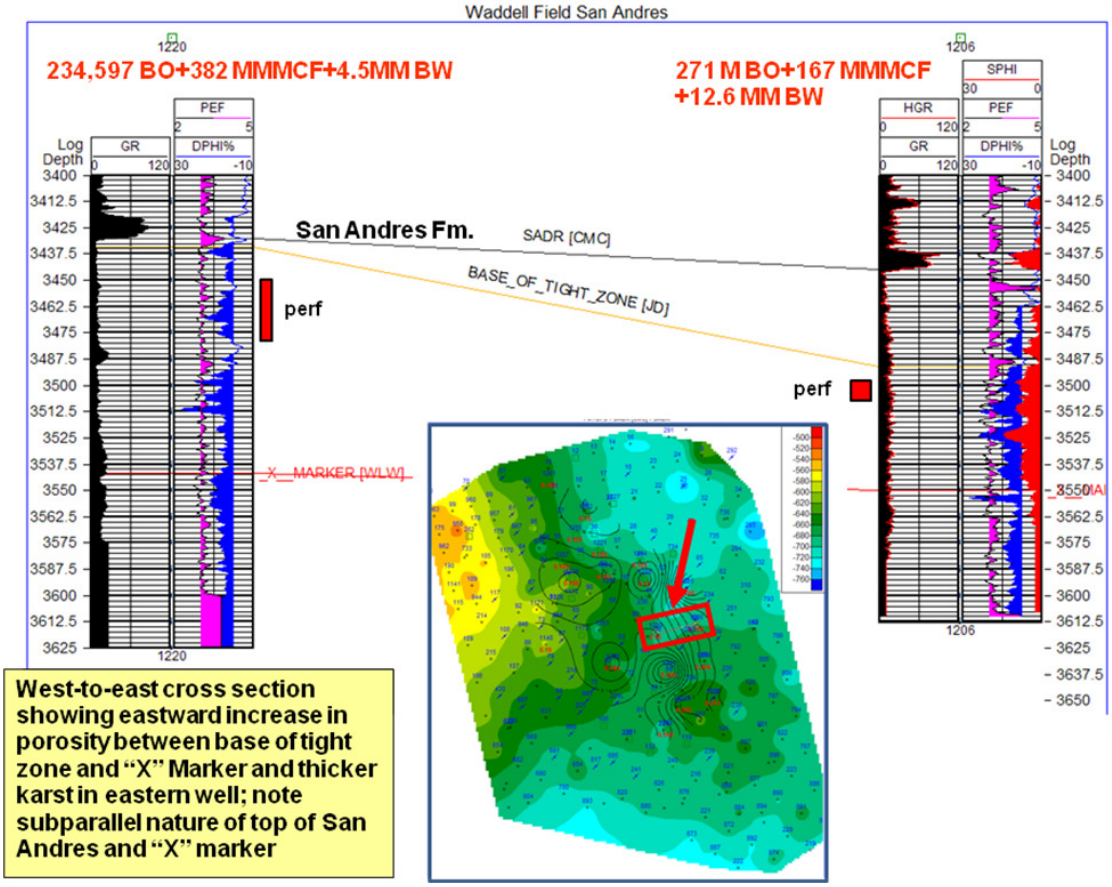

Figure 2.10. Structural wireline log cross section including wells #1220 and #1206. Index map shows top of San Andres structure overlain with P90 porosity contours.

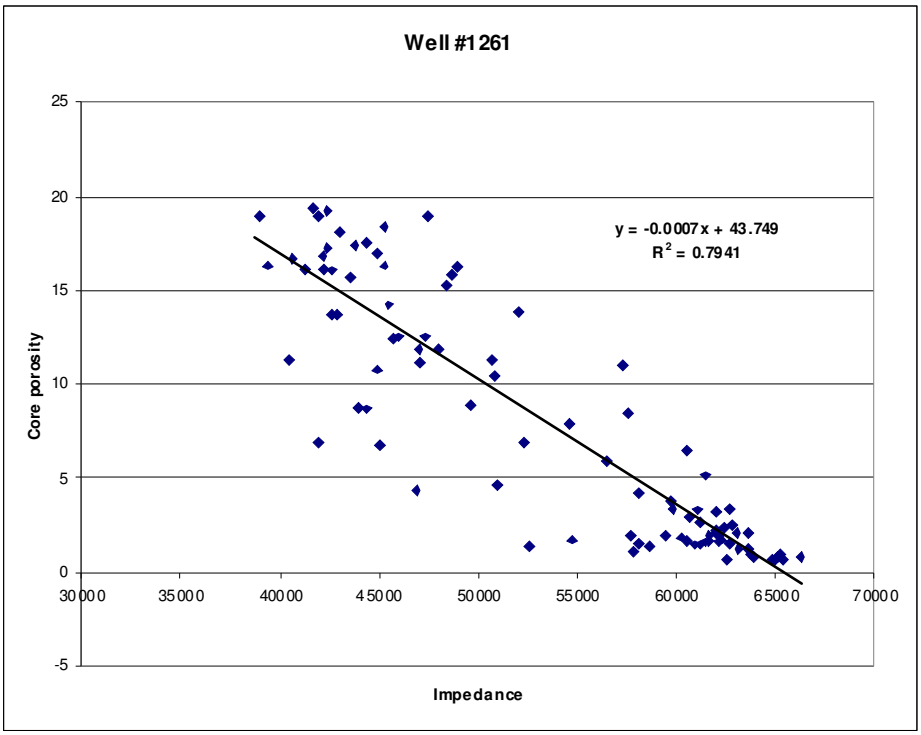

Figure 2.11. Cross plot of core porosity and well log impedance for well #1261.

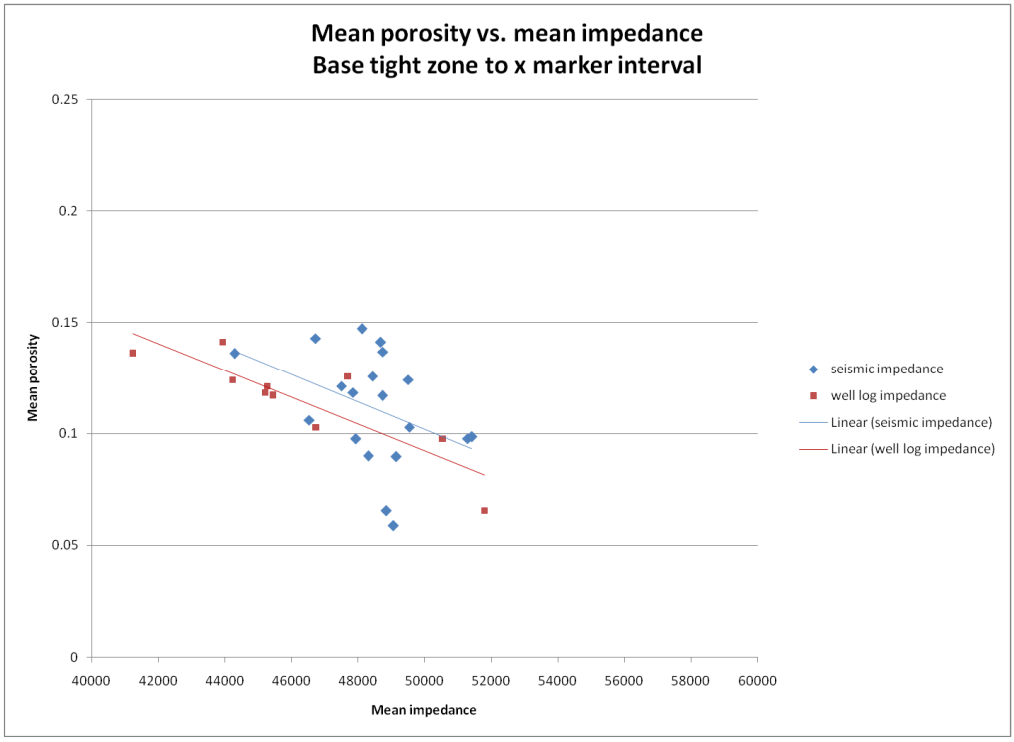

Figure 2.12. Cross plot of mean porosity versus mean impedance from well logs (red) and from seismic data (blue) for the interval between the base of the tight (karst) zone and the "x" marker.

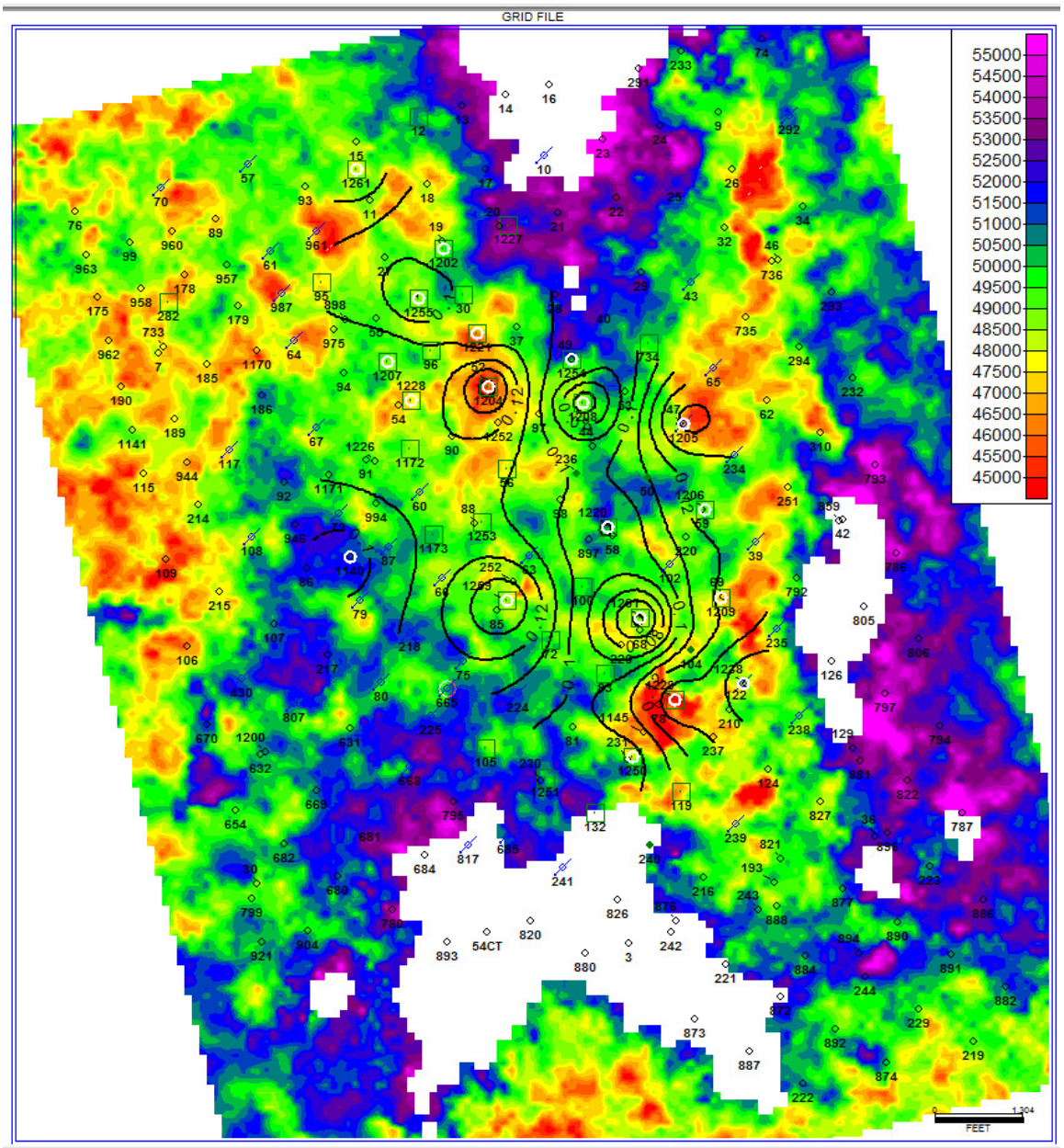

Figure 2.13. Map of mean seismic impedance for the interval from the base of the tight zone to the "x" marker. Mean porosity contours from well logs are superimposed.

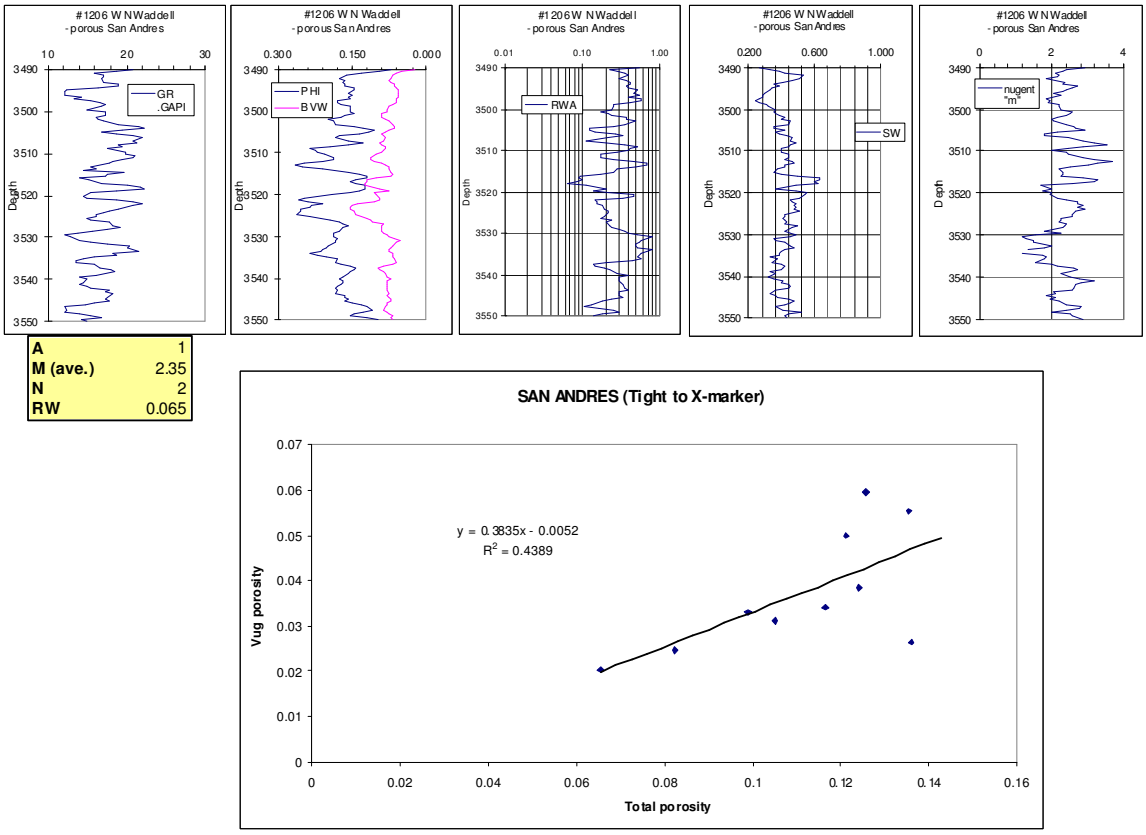

Figure 2.14. Petrophysical profile for well #1206 and cross plot of vug porosity vs. total porosity.

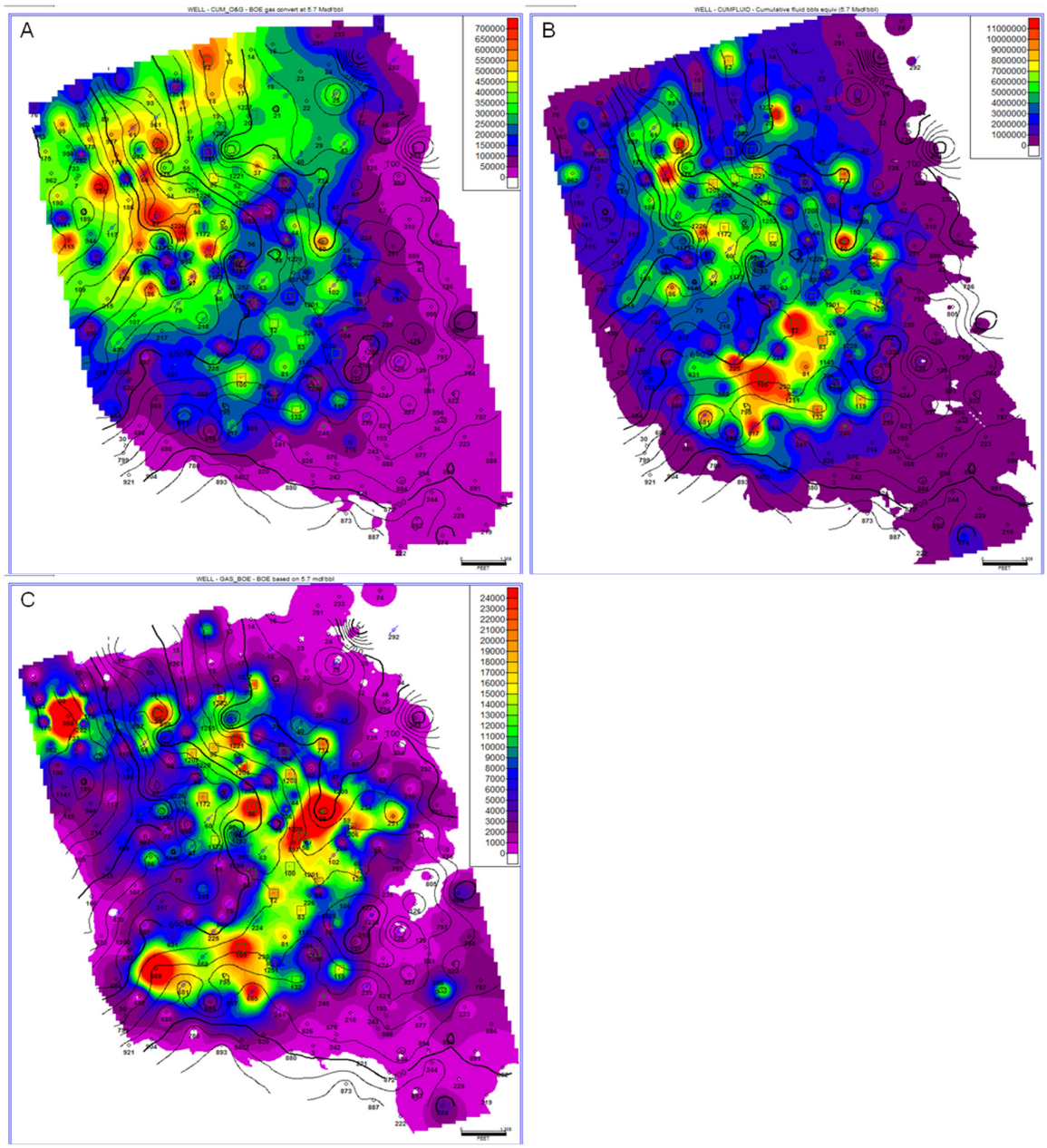

Figure 2.15. A) Cumulative oil and gas map in BOE. B) Cumulative total fluid (oil+gas+water) map in BOE. C) Cumulative gas map in BOE. All maps are superimposed with contours of the top of San Andres subsea depth structure.

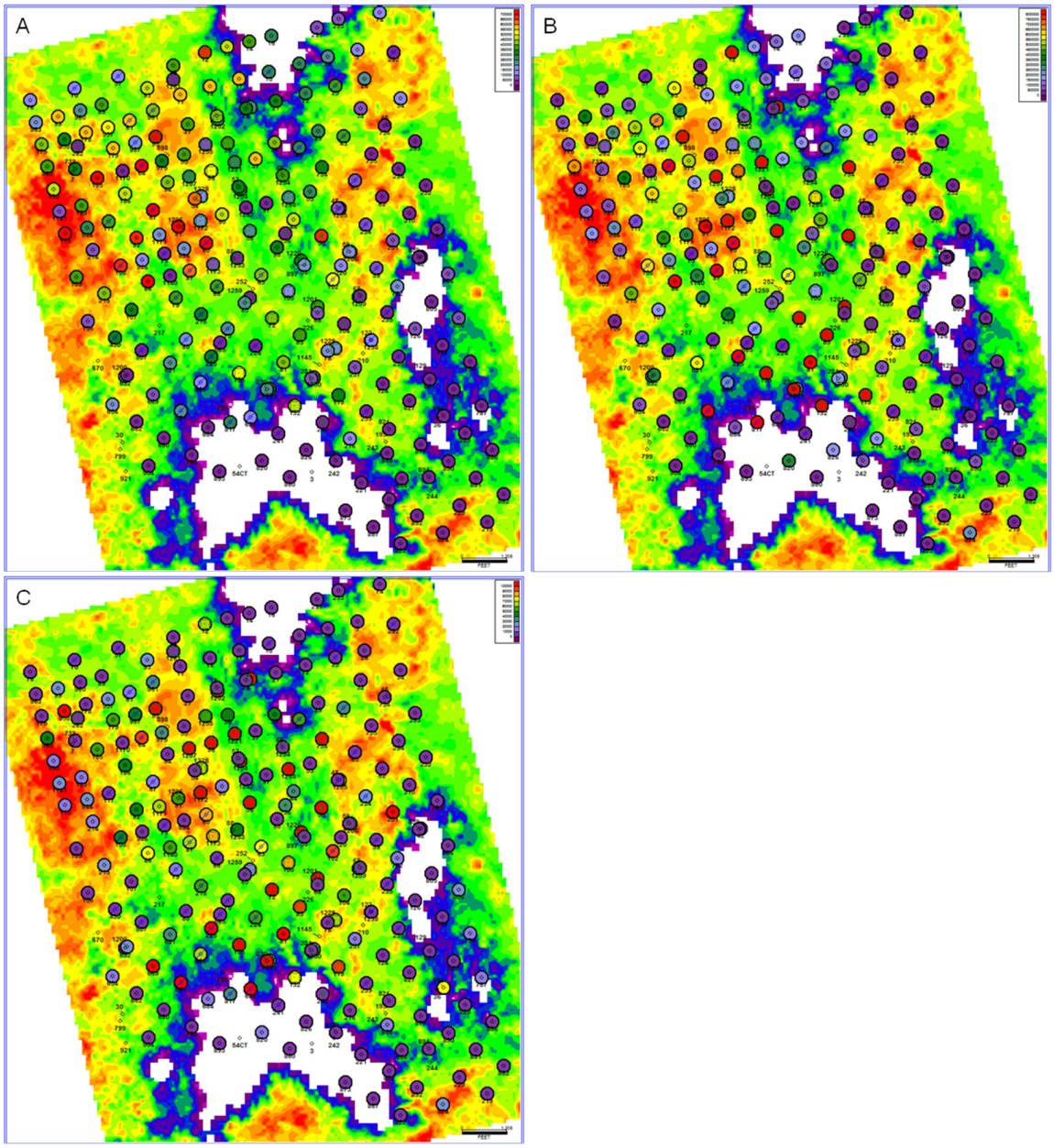

Figure 2.16. Isochron of the reservoir interval from the base of the tight karst zone to the "x" marker overlain by bubbles of A) cumulative oil and gas in BOE; B) cumulative total fluid (oil+gas+water) in BOE; and C) cumulative gas in BOE.

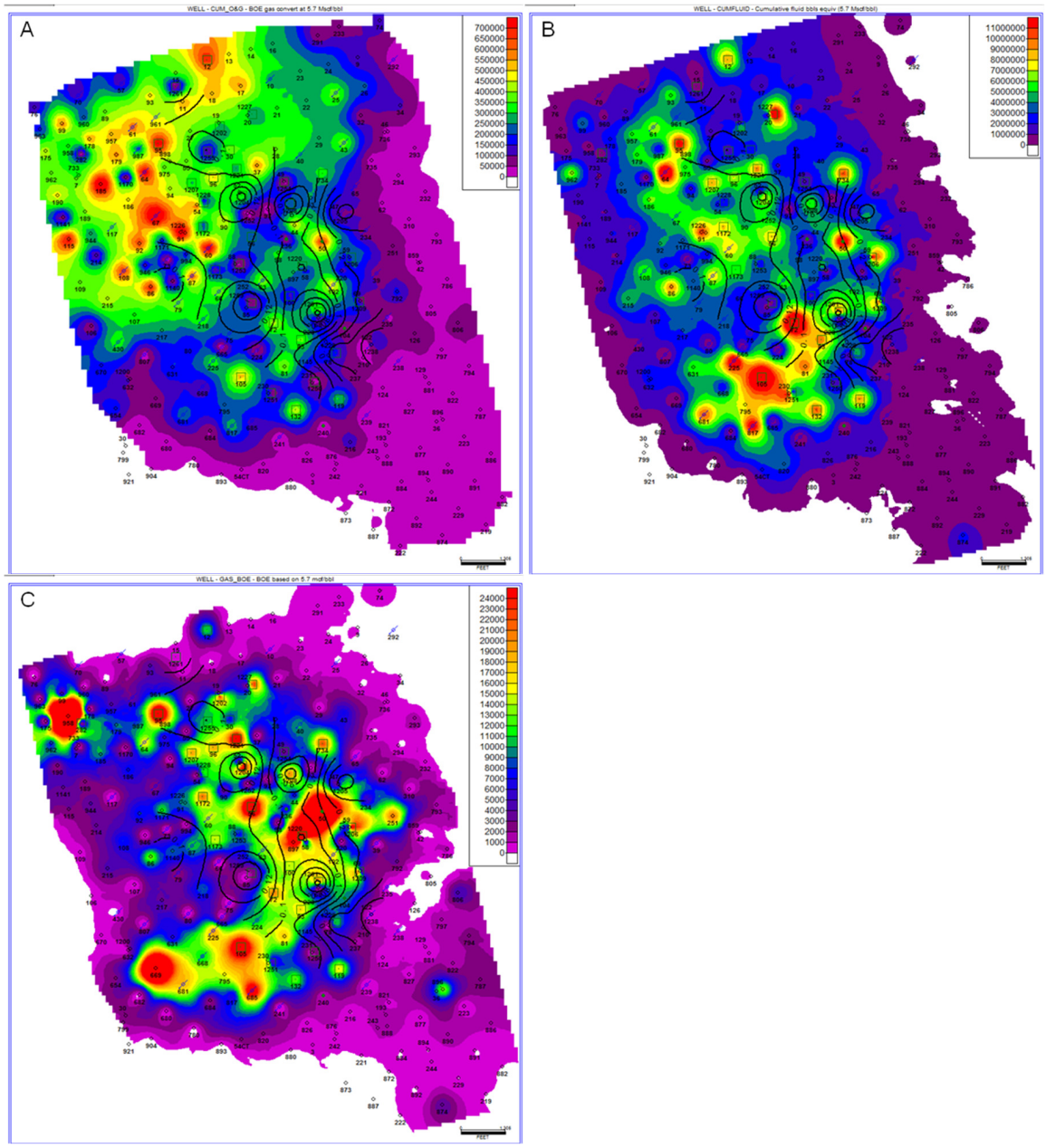

Figure 2.17. A) Cumulative oil and gas map in BOE. B) Cumulative total fluid (oil+gas+water) map in BOE. C) Cumulative gas map in BOE. All maps are superimposed with contours of mean porosity for the base tight to "x" marker interval.

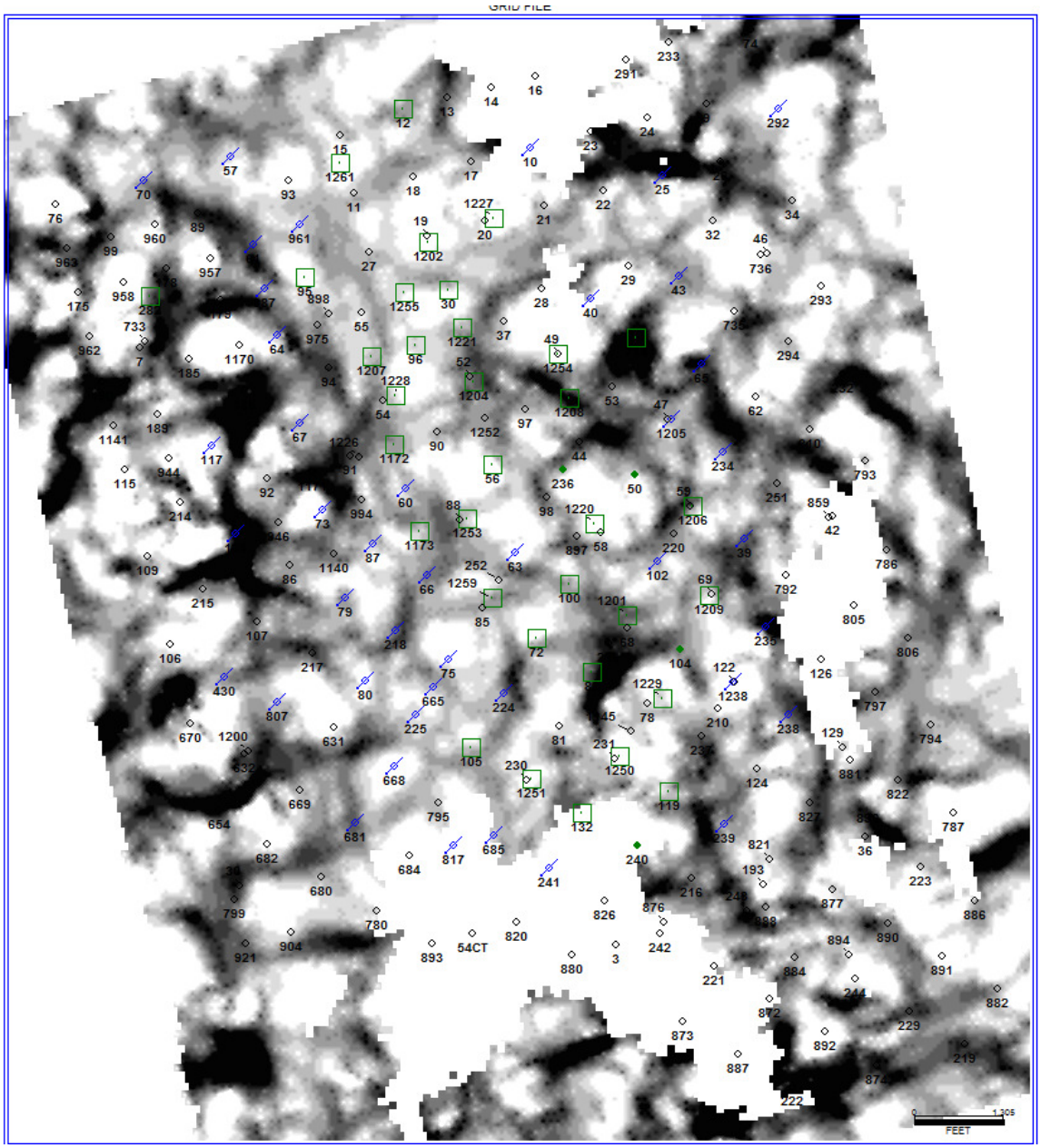

Figure 2.18. Most negative volumetric curvature extracted along the "x" marker horizon.

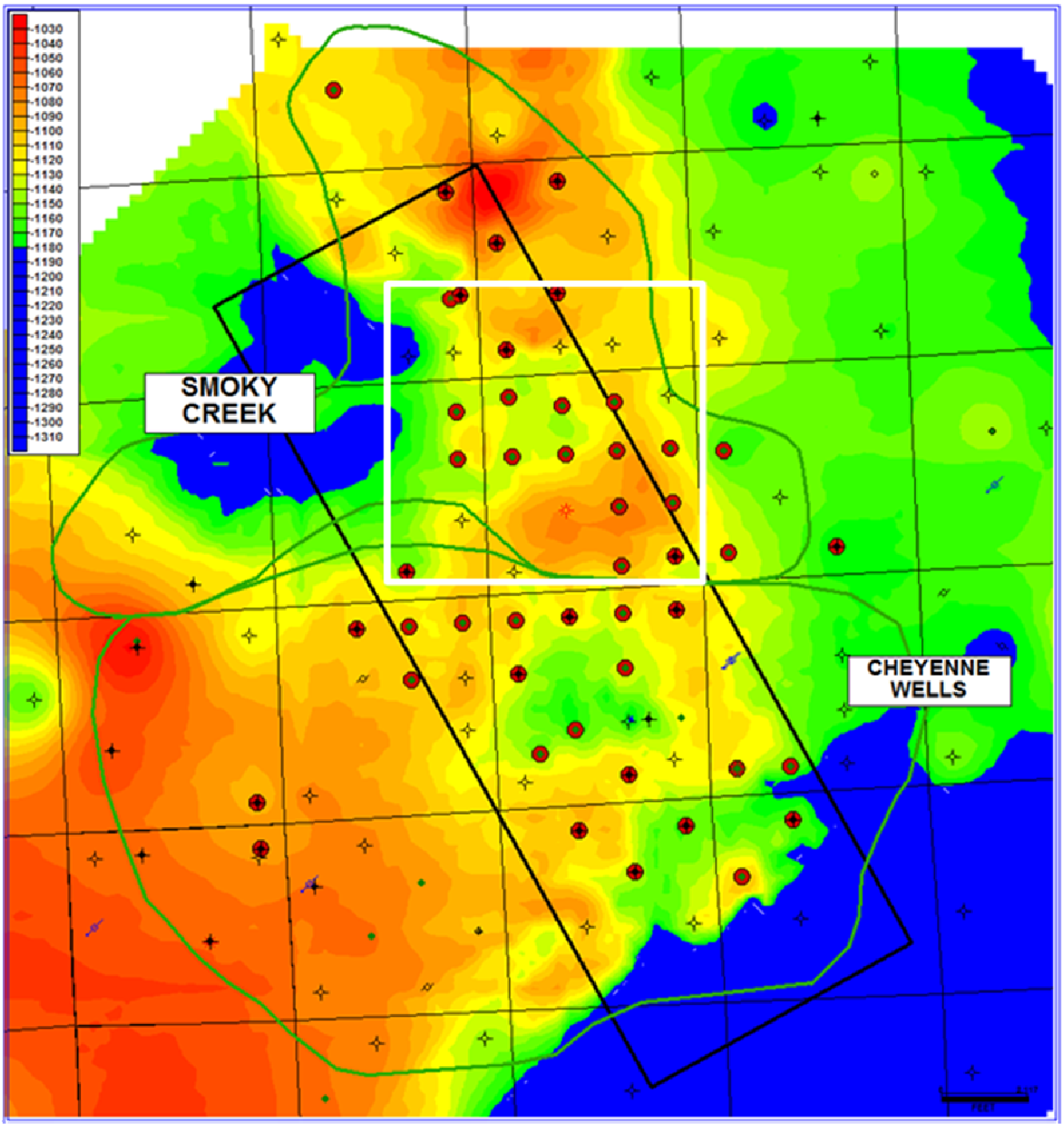

Figure 3.1. Structure map of the top of Spergen in the Mississippian study area, enhanced by seismic control within the 3D seismic outline (heavy black rectangle). Blue fill indicates areas where the top of Spergen is below the oil-water contact. The outlines of the Smoky Creek and Cheyenne Wells fields are shown in green. Wells with Spergen production are highlighted in red. The white box shows the location of Figure 3.2.

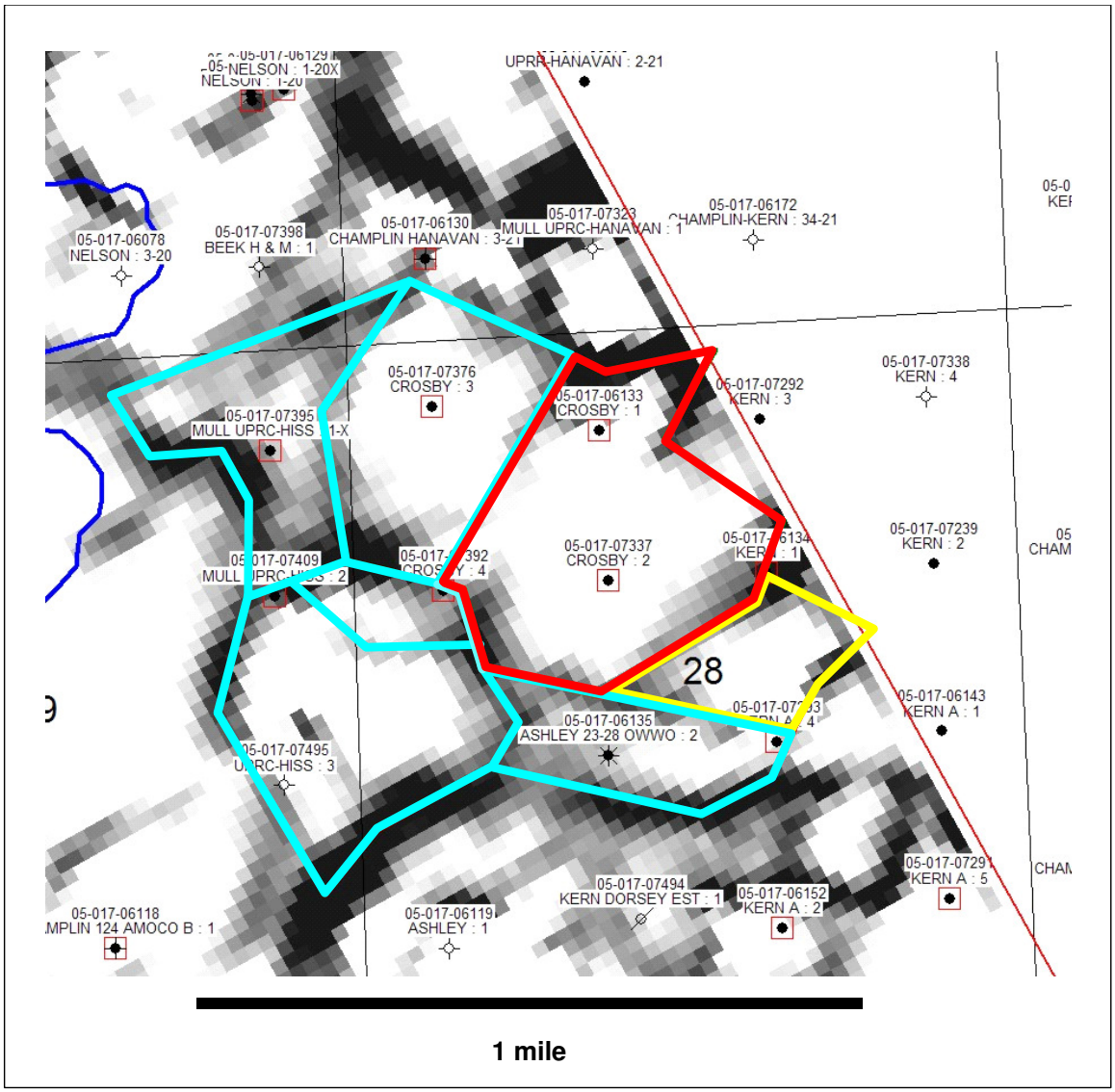

Figure 3.2. Most positive curvature map extracted along the approximate level of the top of Spergen for southern Smoky Creek field. Potential reservoir compartments within the Smoky Creek field based on this curvature map are outlined. Production for the compartment outlined in red has been simulated. The five compartments outlined in blue, which each contain one Spergen producing well, will be simulated during the next reporting period. Note that the yellow compartment contains no wells and may represent untapped reservoir.

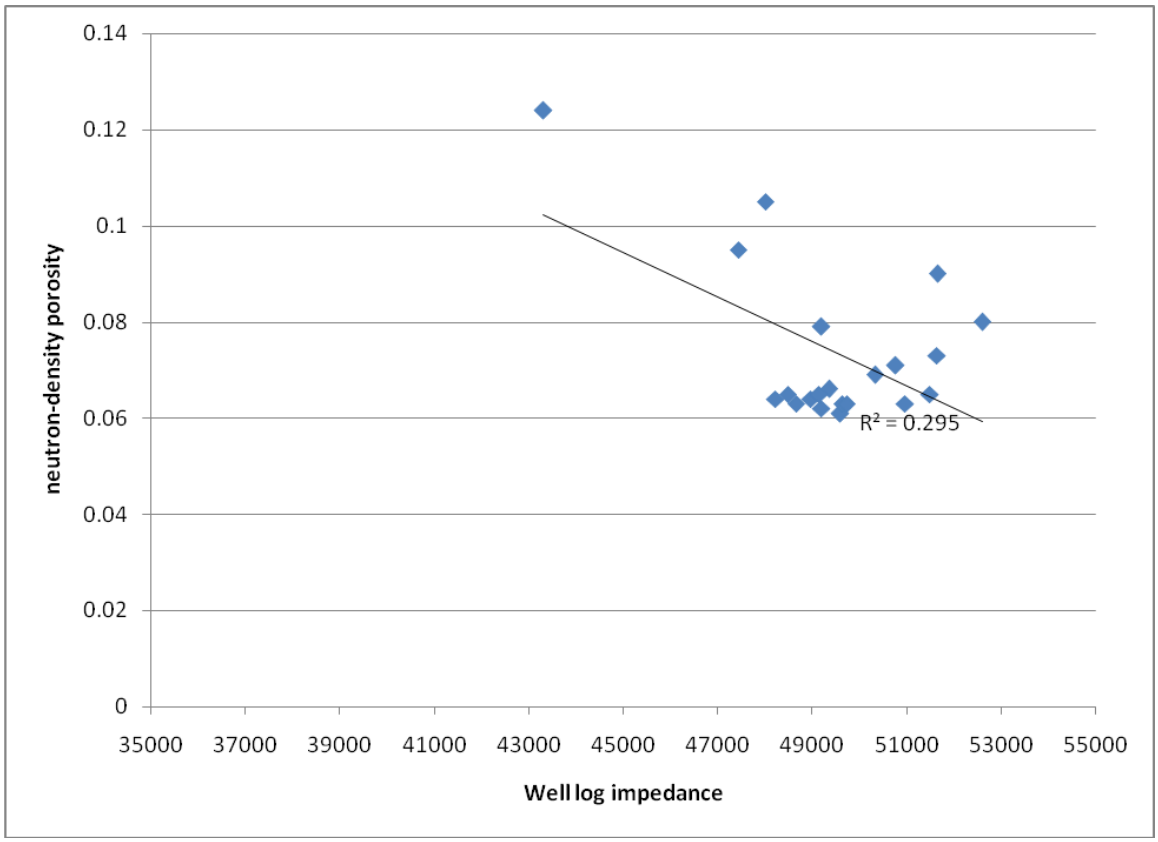

Figure 4.1. Cross plot of neutron-density porosity versus well log impedance in well #1.

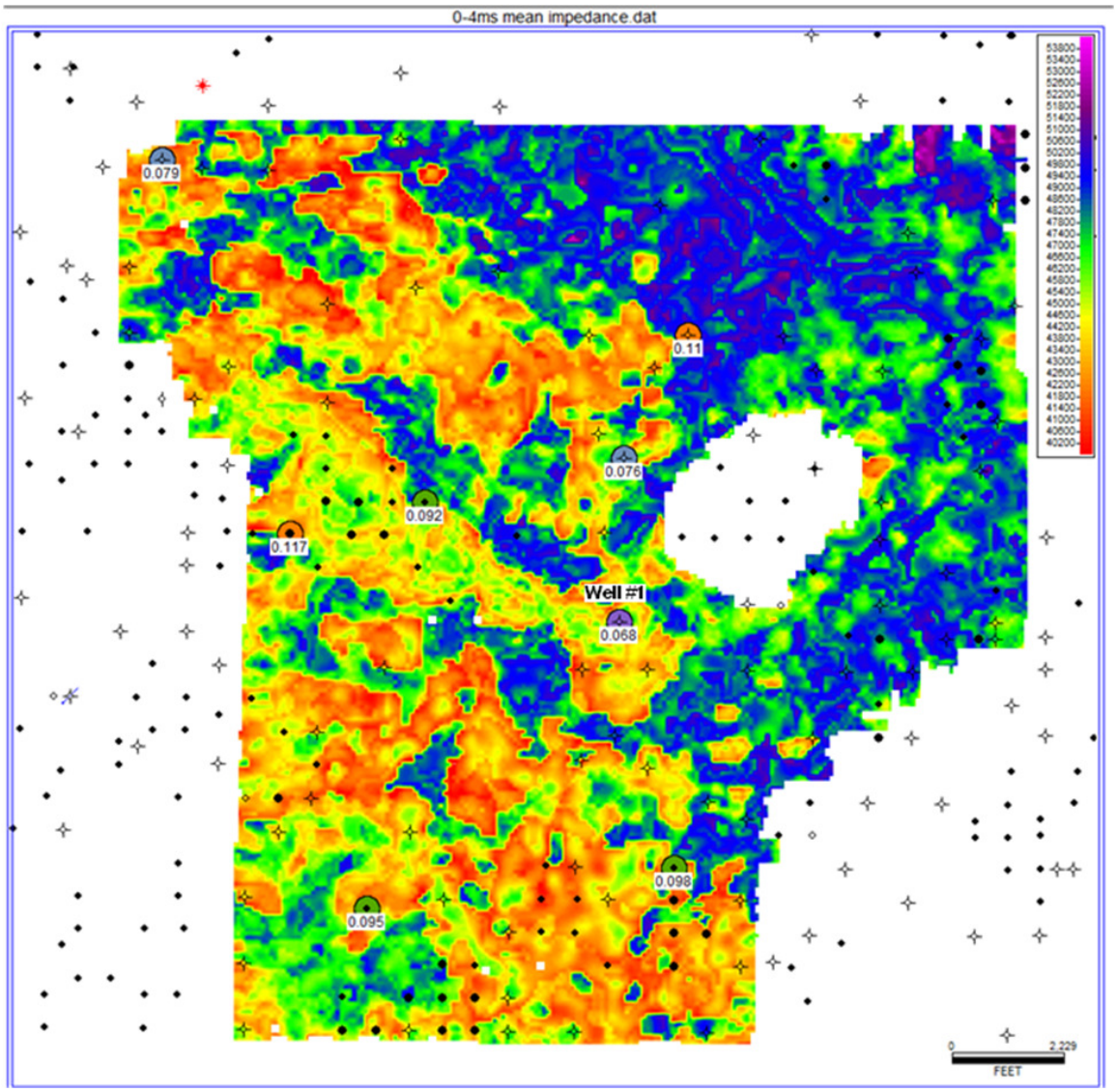

Figure 4.2. Map of mean seismic impedance for the interval from 0 to 4 ms below the top of Arbuckle horizon. Mean porosity from neutron and density logs for the approximately equivalent interval from 0 to 30 ft (9 m) is shown by the colored bubbles, with values annotated. The location of well #1, discussed in the text and Figure 4.1, is shown.

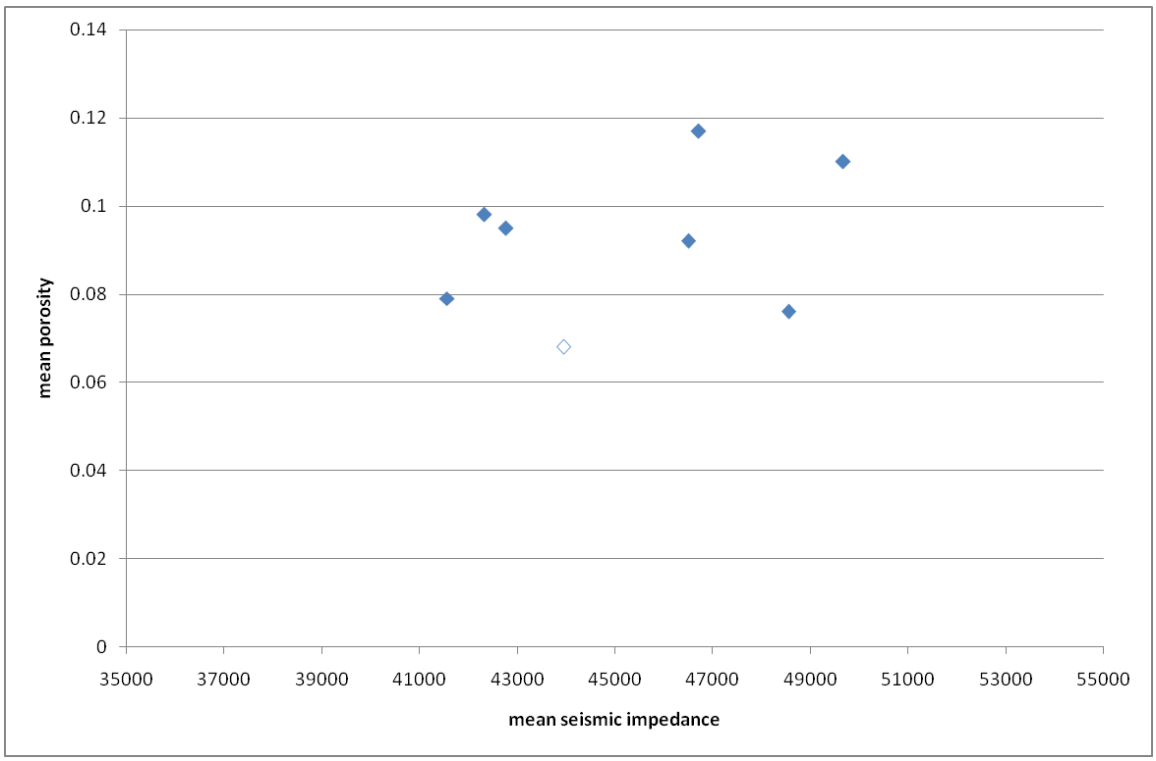

Figure 4.3. Cross plot of mean neutron-density porosity for the interval from 0 to 30 ft (9 m) below the top of the Arbuckle versus mean seismic impedance for the interval from 0 to 4 ms below the interpreted Arbuckle horizon. The open symbol indicates a well that does not penetrate 30 ft (9 m) into the Arbuckle. The average porosity shown for this well is from the top of Arbuckle to the TD of the well. No clear relationship between porosity and impedance is evident from the cross plot.

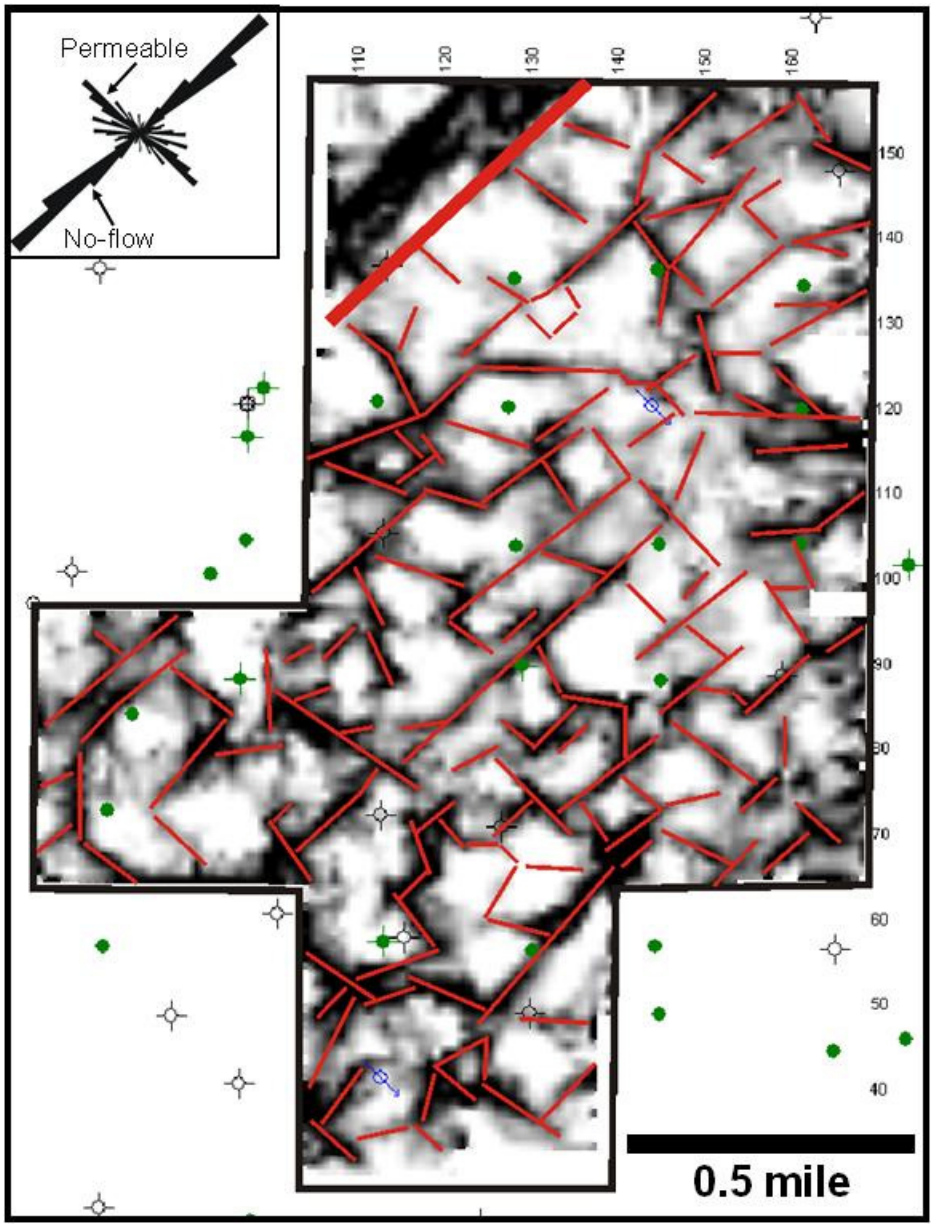

Figure 5.1. Most negative curvature map for the Mississippian in Dickman Field. Interpreted curvature lineaments are overlain in red. The inset shows a rose diagram of lineament orientation.

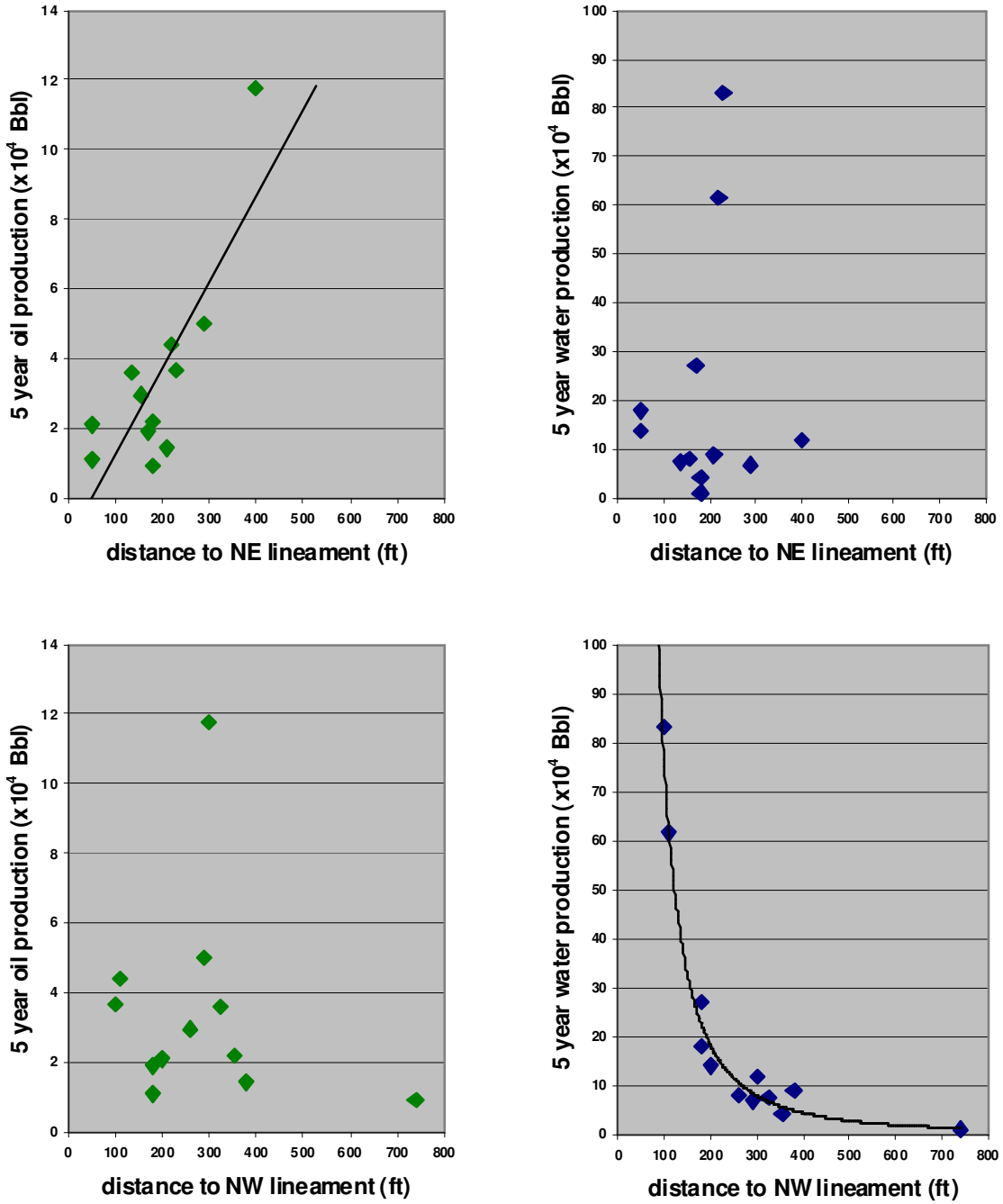

Figure 5.2. Cross plots of 5-year oil (left) and water (right) production versus distance to northeast-trending (top) and northwest-trending (bottom) curvature lineaments.